

Investigation of Magnetic Soils
on the Oak Ridge Reservation, TN

A Thesis Submitted
to the
Temple University Graduate Board

In Partial Fulfillment of the Requirements for the
Masters of Science

By John M. Rivers

August, 2002

Dr. Johnathan Nyquist, Advisor

Dr. Dennis O. Terry, Jr.



Dr. George H. Myer

ABSTRACT

INVESTIGATION OF MAGNETIC SOILS ON THE OAK RIDGE RESERVATION, TN

JOHN M. RIVERS

MASTER OF GEOLOGY

TEMPLE UNIVERSITY, 2002

A 1993, airborne geophysical survey found numerous localized "bull's-eye" magnetic anomalies, apparently of natural origin, associated with dolines on the Oak Ridge Reservation (ORR), Oak Ridge, Tennessee. Susceptibility measurements made on a soil core extracted from one such doline located on Copper Ridge (Anomaly B) showed the soil to be magnetic throughout the soil profile (average susceptibility $>200 \times 10^{-5}$ S.I. units), while a soil core removed from outside the doline showed an average susceptibility of less than 20×10^{-5} S.I. units. Pedologic characterization of the soil cores both inside and outside of the doline showed a series of stacked soil profiles, all in the early stage of pedogenesis, with A-horizons lying directly on C-horizons that were transforming to Bw-horizons, indicating periodic burial by fresh colluvium or alluvium. Based on mottling seen throughout the soil cores, which is evidence of hydromorphy, I identified the soils as aquepts using the USDA soil classification. In the majority of the soil profiles the magnetic susceptibility peaked at the base of the A-horizons.

I investigated nine different mechanisms discussed in the literature for the formation of magnetic soil. I used scanning electron microscopy (SEM), energy dispersive X-ray (EDX), and X-ray diffractometry (XRD), to supplement pedologic characterization. Based on the XRD results, the source of the soil magnetism was identified as the ferromagnetic mineral, maghemite. SEM measurements showed that the magnetic particles extracted from the soil cores were too large and rounded to be biogenic maghemite. Apparently the maghemite formed by anaerobic microbial iron reduction followed by the formation of maghemite, or by abiological weathering and reduction of an iron-bearing mineral followed by oxidation.

Maghemite occurs in the soil both inside and outside of the magnetic anomaly, but was found in higher concentrations inside the anomaly. EDX analysis showed that the soil core extracted from inside the magnetic anomaly contained more iron than the core extracted outside the anomaly, suggesting a different parent material for the soil inside the doline. ORR reports and soil maps indicate that the parent material is an ancient alluvium. Ancient alluviums found on the ORR have more iron as a result of the weathering of iron rich sediment deposited by an ancient river. Through topographic inversion these ancient alluviums are now found on top of Copper Ridge.

I found evidence to support an alluvial source for the soil inside the doline, including rounded metaquartzite and illite (weathered biotite). I conclude that soils derived from ancient alluviums have accumulated in dolines on the ORR and that hydromorphy within the dolines has increased the maghemite concentration.

The magnetic anomalies detected by the airborne geophysical survey resulted from a combination of increased soil thickness in the dolines, and the higher maghemite concentration that developed in these iron rich soils.

Table of Contents

| | |
|---------------------------------------------------------------------------|------|
| Abstract..... | ii |
| List of Tables | viii |
| List of Figures | ix |
| List of Appendices..... | x |
| Acknowledgements | xip |
| Chapter 1 Background..... | 1 |
| Introduction..... | 1 |
| Oak Ridge Geology..... | 6 |
| Oak Ridge Geomorphology, Karst and Topographic inversion | 9 |
| Oak Ridge Reservation Soils | 11 |
| Discovery of Magnetic Soils on the Oak Ridge Reservation | 18 |
| Magnetic Properties of Minerals..... | 24 |
| Maghemite in Soils | 28 |
| Hypotheses Proposed | 33 |
| Chapter 2 Soil Core Characterization..... | 35 |
| Introduction..... | 35 |
| Procedure..... | 36 |
| Thin Section Preparation..... | 37 |
| Thin Section Analysis | 42 |
| Characterization of the Soil Core Taken Inside the Magnetic Anomaly | 44 |
| Horizon Designation and Soil Classification | 44 |
| Soil Genesis | 47 |

| | |
|----------------------------------------------------------------------|----|
| Magnetic Susceptibility of Soil | 49 |
| Summary | 52 |
| Characterization of the Soil Core from Outside Magnetic Anomaly..... | 52 |
| Horizon Designation and Soil Classification | 52 |
| Soil Genesis | 53 |
| Magnetic Susceptibility of Soil | 54 |
| Summary | 55 |
| Chapter 3 Lab Analysis of Soil Cores for Anomaly B..... | 58 |
| Transmission Electron Microscopy | 58 |
| Purpose..... | 58 |
| Grid Preparation..... | 58 |
| Results | 59 |
| Scanning Electron Microscopy | 60 |
| Introduction | 60 |
| Sampling..... | 61 |
| Sample Preparation | 62 |
| Observations | 63 |
| Discussion..... | 66 |
| X-Ray Diffraction | 69 |
| Introduction | 69 |
| Sampling..... | 70 |
| Results | 71 |
| Summary | 73 |

| | |
|------------------------------------------------------------------|-----------|
| Chapter 4 Discussion and Conclusions | 74 |
| Evaluating the Mechanisms of Magnetic Soil Formation..... | 74 |
| Sources of Iron..... | 79 |
| The Influence of Karst..... | 83 |
| Conclusions..... | 84 |
| Implications and Recommendations for Further Work..... | 84 |
| Bibliography..... | 87 |
| Plate 1 | 91 |
| Plate 2 | 92 |
| Plate 3 | 93 |
| Appendices..... | 94 |

LIST OF TABLES

| | |
|----------------------------------------------------------------------------------------------------|----|
| Table 1: Properties of the soil core inside the magnetic anomaly..... | 45 |
| Table 2: Properties of the soil core outside the magnetic anomaly..... | 54 |
| Table 3: Sample numbers, descriptions, and weights of Scanning Electron Microscopy samples..... | 61 |
| Table 4: Minerals identified using X-Ray Diffraction..... | 71 |

LIST OF FIGURES

| | |
|--------------------------------------------------------------------------------------------------------------------------------------------------|----|
| Figure 1: Study area showing the location of the Oak Ridge Reservation in Tennessee..... | 2 |
| Figure 2: Aerial view of the Oak Ridge Reservation..... | 3 |
| Figure 3: Location of the Oak Ridge Reservation in the southern Appalachian Valley and Ridge Province of eastern Tennessee..... | 7 |
| Figure 4: Stratigraphic section in Melton Valley and Copper Ridge..... | 8 |
| Figure 5: Topographic Inversion..... | 10 |
| Figure 6: Soil order distribution on the Oak Ridge Reservation..... | 13 |
| Figure 7: The distribution of soils on Copper Ridge..... | 14 |
| Figure 8: Percentage of soil orders on the Oak Ridge Reservation by Area..... | 15 |
| Figure 9: Magnetic gradient of the Oak Ridge Reservation and ORR facilities..... | 19 |
| Figure 10: Magnetic Anomalies on Copper Ridge..... | 20 |
| Figure 11: Magnetic profile from Anomaly..... | 22 |
| Figure 12: Magnetic susceptibility from cores drilled on Copper Ridge..... | 23 |
| Figure 13: Magnetic gradient in relation to topography..... | 25 |
| Figure 14: Soil Core Description..... | 38 |
| Figure 15: Diagram of the third core tube extracted within the magnetic anomaly showing horizon changes and magnetic susceptibility..... | 51 |
| Figure 16: Diagram of the second core tube extracted outside of the magnetic anomaly showing horizon changes and magnetic susceptibility..... | 57 |
| Figure 17: Magnetic anomalies of Oak Ridge overlain by ancient alluvium..... | 82 |

LIST OF APPENDICES

| | |
|----------------------------------------------------------------------------------|-----|
| Appendix 1: Diagrams of Anomaly B soil core with magnetic susceptibilities | 94 |
| Appendix 2: Horizon description data..... | 107 |
| Appendix 3: Energy dispersive x-ray plots | 115 |
| Appendix 4: Society of Exploration Geophysicists extended abstract | 131 |

ACKNOWLEDGEMENTS

Thanks to the Temple geology staff including Shelah Burgess, Roger Cutitta and Donald Deighkai for providing a friendly and efficient working environment. I am grateful to Steve Widing and the Temple Biology Department for training and use of their transmission electron microscope and sorry about the filaments. Dr. William Doll, Les Beard and Jeff Garney are appreciated for their hospitality at Oak Ridge and for provision of much of the data presented in this thesis. Dr. Yul Roh took a week of his time instructing me in the use of SEM and EDX. Dr. Roh also provided all XRD data presented in this thesis. Without his efforts this work could not have been completed. Thanks to my fellow graduate students for their support in the creation of this thesis especially Christine Metzger and Matthew Weikel for technical support and Matt McCoy for emotional support. I received valuable insight from Dr. George Myer and Dr. Dennis Terry. They made learning fun and that is what this is all about. Special thanks to Dr. Jonathan Nyquist for the extraordinary efforts he has made to keep me on track and in focus. He has shown great patience to me and used laughter to make some tough but valid points. Under his tutelage I have become a scientist. Finally, I appreciate my students for teaching me and my friends and family for supporting me.

CHAPTER 1 BACKGROUND

Introduction

In the early 1990s, an airborne geophysical instrument package was employed in an effort to map known waste areas and locate any unknown waste areas on the Oak Ridge Reservation, Oak Ridge, TN. The Oak Ridge National Laboratory (ORNL) and the Oak Ridge Reservation (ORR) where the laboratory is located, is located 50 miles west of Knoxville, Tennessee (Figures 1 and 2). The laboratory was first established during World War II as part of the Manhattan Project. Nuclear research lead to radioactive waste disposal on the Oak Ridge Reservation. Early disposal typically consisted of placing waste in metal canisters and burying these in trenches. Records of the burial sites were minimal and many were lost. Recent concerns about incomplete records prompted the airborne geophysical survey used to locate these waste sites, as environmental restoration has become a priority at ORNL. The airborne instrument package used in this effort included a pair of magnetometers used in tandem to produce a magnetic gradient map of the ORR.

Oak Ridge researchers interpreted the magnetic anomalies using aerial photographs and, where needed, site inspection. They found no major new waste sites, however they did find magnetic anomalies not associated with waste sites. These were bull's-eye shaped anomalies over sites that displayed no evidence of anthropogenic disturbance. Magnetic susceptibility measurements of topsoil samples proved that the bull's-eye anomalies were centered on concentrations

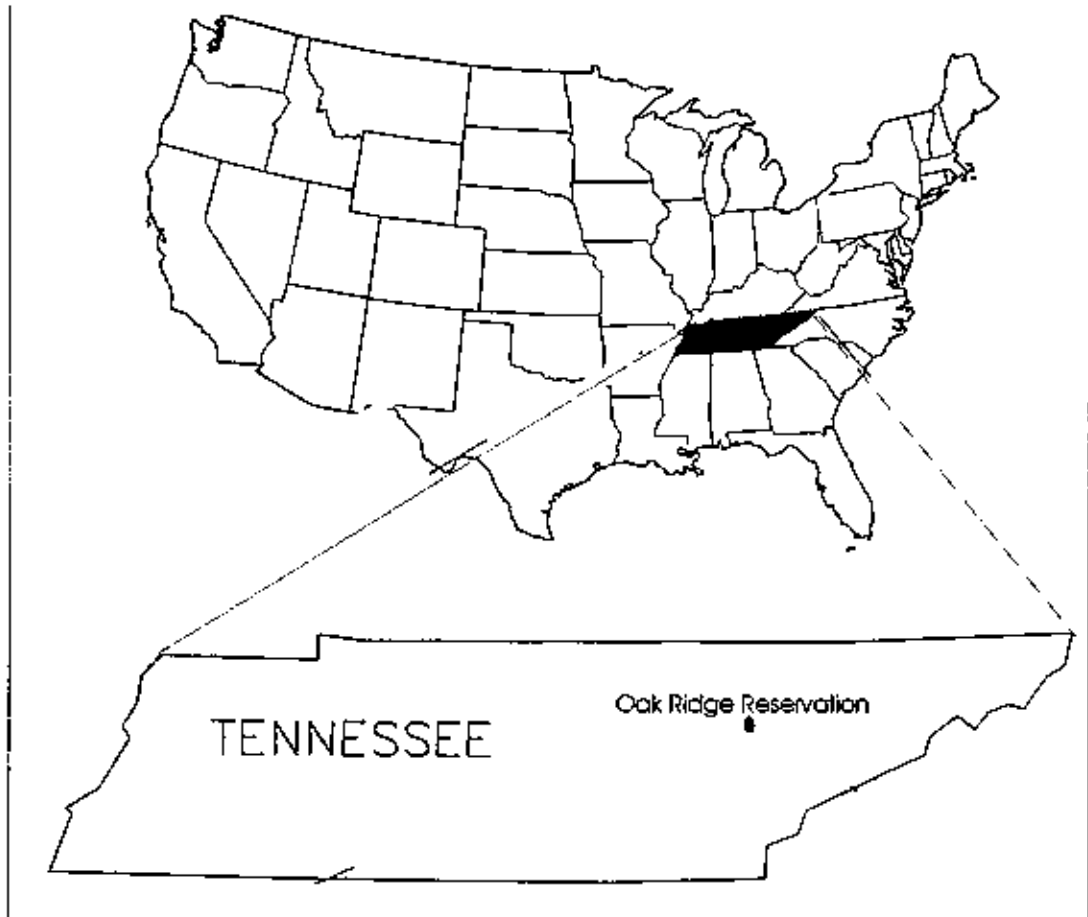


Figure 1: Study area showing the location of the Oak Ridge Reservation in Tennessee from (Drumm et al., 1990).

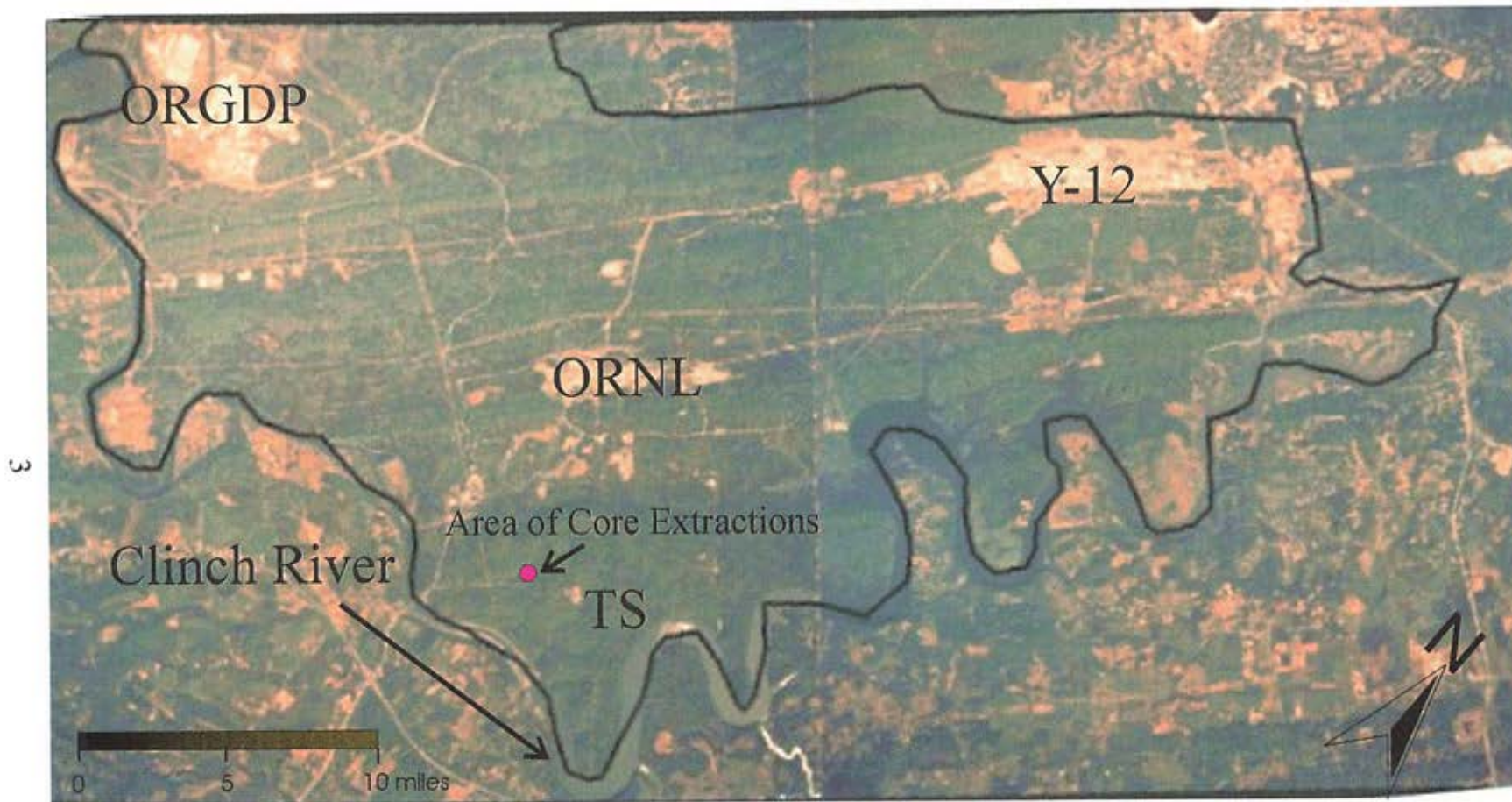


Figure 2: Aerial view of the Oak Ridge Reservation showing facilities; Oak Ridge Gaseous Diffusion Plant (ORGDP), Y-12 weapons plant (Y-12), Oak Ridge National Laboratories (ORNL), Tower Shielding (TS). The magnetic cores were extracted near the tower shielding facility (Photo courtesy of the Oak Ridge Environmental Restoration Program).

of highly magnetic soil. This raised questions about the utility of airborne magnetics to detect buried waste and of our ability to differentiate between magnetic anomalies created by buried hazardous waste and harmless magnetic soils.

In 1996, Oak Ridge researchers collected two soil cores associated with a large magnetic anomaly, in an attempt to explain the bull's-eye pattern and to ascertain the depth of the magnetic soils. One soil core was taken from inside the anomaly and one from outside the anomaly. Magnetic susceptibility measurements of both cores showed the soil inside the anomaly to have an average susceptibility of greater than 200×10^{-5} S.I. units to a depth of more than 50 ft, and the soil taken outside the anomaly to have an average susceptibility of less than 20×10^{-5} S.I. units to a depth of 15 ft. Study of the magnetic core showed its greatest susceptibility in the top 5 ft. While the overall susceptibility of the core diminished with depth, localized susceptibility peaks could be found to a depth of 20 ft. The origin of this magnetism was unknown as the magnetic soil rested on nonmagnetic dolostone. The mineral maghemite, a magnetic iron oxide, had been discovered in soils on other parts of the ORR (Lee et al., 1984; Hatcher et al., 1992; Kopp and Lee, 1987) but had not yet been identified in the soil at this site.

In this thesis, I identify the magnetic minerals in the soil cores collected in 1996 and show how these minerals were produced on nonmagnetic bedrock. A pedologic characterization of the soil cores explains the susceptibility patterns in the magnetic core, correlates changes in magnetic susceptibility with soil

horizons, and defines the differences between the soil located inside and outside the anomaly. Finally, I analyze the location of the bull's-eye anomalies in light of the topography, structure and soil distribution of the ORR.

Oak Ridge Geophysical Survey

Magnetic, electromagnetic, and radiometric airborne geophysical data were collected by the Oak Ridge Environmental Science division at the ORR in January, 1993 in an attempt to use geophysical methods originally developed for mineral and oil exploration to locate metallic storage drums used as containers for buried waste (Doll et al., 2000). A 158 ft cable, suspended from a helicopter, held two cesium vapor magnetometers (95 ft below the helicopter), a global positioning system (127 ft below the helicopter), and an electromagnetic system (158 ft below the helicopter). The instruments were suspended by cable in order to minimize the effect of the helicopter on the measured fields. The electromagnetic system was flown 95 ft above the ground to avoid treetops. Flight lines (NNW-SSE) were oriented perpendicular to geologic contacts and separated by an average of 475 ft. A reading was taken approximately every 8 ft. The survey was flown in a "draped" manner to maintain a constant altitude above the ground (Nyquist and Doll, 1996).

The two magnetometers were vertically separated by 9.8 ft allowing for the measurement of magnetic gradient, which is calculated by subtracting the magnetic field measured by the two magnetometers and dividing by the distance between them. Magnetic gradient data are useful because differencing the two

readings negates regional magnetic trends and sources of noise such as diurnal fluctuations of the earth's magnetic field. Taking the magnetic gradient also improves the resolution of closely spaced anomalies because it yields narrower peaks over sources. The pair of magnetometers were suspended 95 ft below the helicopter to minimize the effect the helicopter on the measured field.

During this survey magnetic bull's-eye anomalies were discovered in association with soils overlying the Copper Ridge Dolomite (CRD), within which there was no known waste disposal. Many of the soil-related magnetic bull's-eyes were detected by multiple flight lines, so it is unlikely these anomalies were the product of noise or instrument path variations. These anomalies had magnetic readings ranging from 0.06-0.5 nT/m at an altitude of 158 ft (Doll et al., 1995). Oak ridge researchers were unsure why such anomalies overlay ORR geology, made up mostly of shale and dolostone.

Oak Ridge Geology

The ORR lies in the southern portion of the Appalachian Valley and Ridge province (Figure 3). Thrust sheets, striking 53° NE and dipping 35° SE, that formed in the Paleozoic, make up the ORR structure (Lee et al., 1984; Hatcher et al., 1992). The Copper Ridge thrust sheet, which forms the ridges of the ORR, is bounded by the Copper Creek and Beaver Valley thrust faults.

The three main stratigraphic groups that form the thrust sheets are: the Conasauga Group (Cambrian), the Knox Group (Upper Cambrian-Lower Ordovician), and the Chickamauga Group (Middle-Upper Ordovician) (Figure 4). The Conasauga Group is comprised mainly

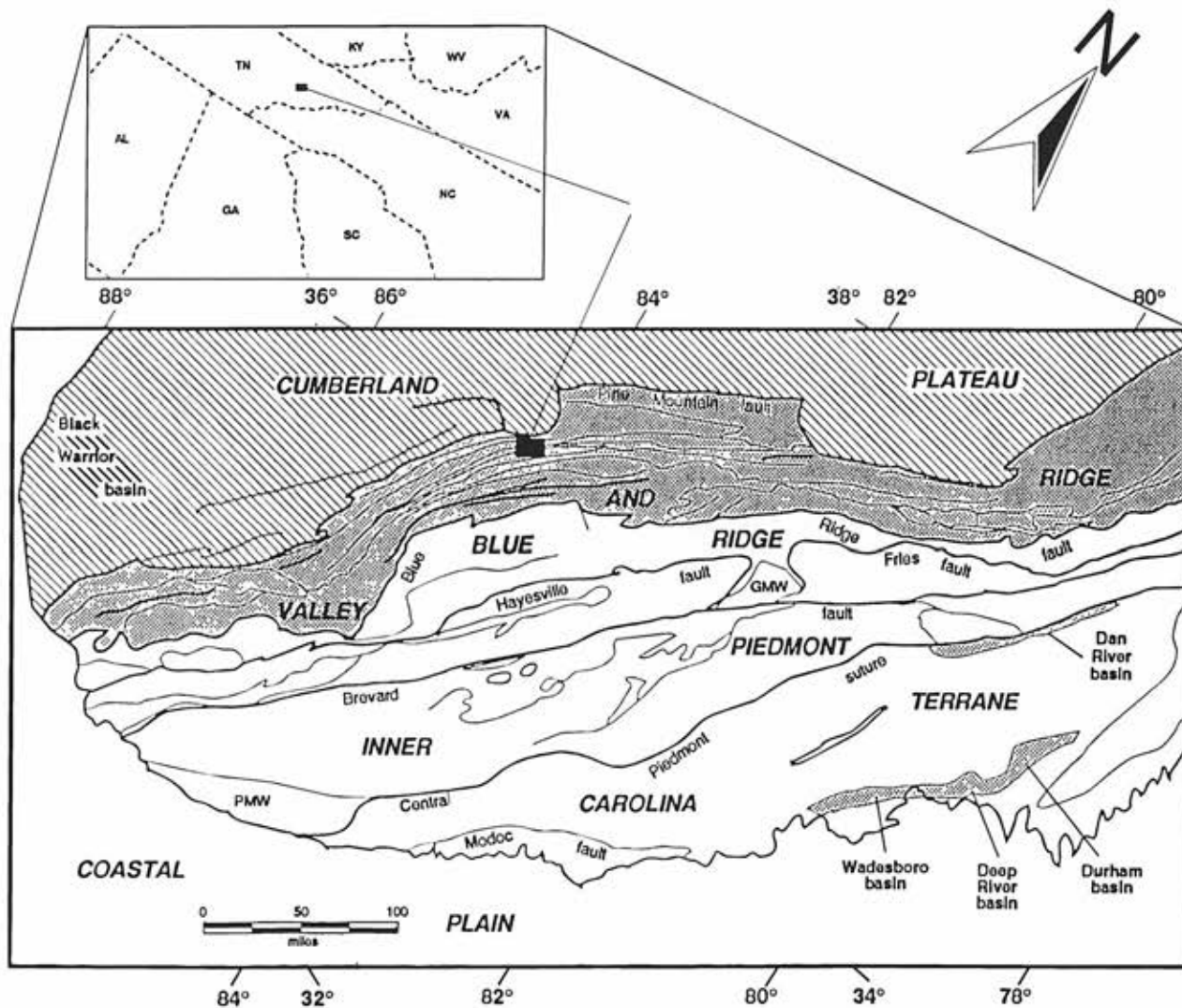


Figure 3: Location of the Oak Ridge Reservation in the southern Appalachian Valley and Ridge Province of eastern Tennessee. PMW - Pine Mountain window, GMW - Grandfather Mountain window, SMW - Sauratown Mountain window (from Hatcher et al., 1992).

| | | Lithology | Thickness, m | Formation | Structural Characteristics | Hydrologic Unit |
|------------|--------|-----------|-------------------------|--------------------------------------------------------------------------|---------------------------------|-----------------|
| ORDOVICIAN | UPPER | | 100-170 | Omc Moccasin Formation | Weak unit Upper décollement | Aquifer |
| | | | 105-110 | Owl Witten Formation | | |
| | | | 5-10 | Obr Bowen Formation | | |
| | MIDDLE | | 110-115 | Obe Benboit / Wardell Formation | Aquifer | |
| | | | 80-85 | Ork Rockdell Formation | | |
| | | | 75-80 | Ofl <small>Hogskin Member</small> Roanor Shale Member | | Aquifer |
| | | | 70-80 | Oe <small>Unadilla Fm</small> Edson Member Obl Blackford Formation | | |
| | LOWER | | 75-150 | Oma Mascot Dolomite | Strong units Ramp zone | Aquifer |
| | | | 90-150 | Ok Kingsport Formation | | |
| | | | 40-60 | Olv Longview Dolomite | | |
| 152-213 | | | Oc Chepultepec Dolomite | | | |
| CAMBRIAN | UPPER | | 244-335 | Cor Copper Ridge Dolomite | Aquifer | |
| | | | 100-110 | Emn Maynardville Limestone | | |
| | MIDDLE | | 150-160 | Cn Nolichucky Shale | Weak units Basal décollement | Aquifer |
| | | | 98-125 | Cdg Dismal Gap Formation (Formerly Maryville Ls.) | | |
| | | | 25-34 | Crg Rogersville Shale | | |
| | | | 31-37 | Cf Friendship Formation (Formerly Rutledge Ls.) | | |
| | LOWER | | 56-70 | Cpv Pumpkin Valley Shale | | |
| | | 122-183 | Cr Rome Formation | | | |

- Shale
- Limestone
- Chert
- Dolostone
- Sandstone

Figure 4: Stratigraphic section of Melton Valley and of Copper Ridge on the ORR. Copper Ridge Dolomite is the highest topographic unit on both Copper and Chestnut Ridges. Susceptibility measurement of cores showed that these formations have low magnetic susceptibilities (from Hatcher et al., 1992).

of shales and is a valley-former. Both the Knox and the Chickamauga Groups are comprised mostly of limestone. The Knox Group is more resistant to weathering and stands topographically higher than the Chickamauga Group. The most resistant member of the Knox group is the Copper Ridge Dolomite. The Copper Ridge Dolomite, which forms a local topographic high, is a source of erosional materials. It is described as “a massively bedded cherty dolomite, commonly forming ridges in the Valley and Ridge province of the Appalachians, and characterized by the presence of bedded oolitic chert” (Doil et al., 1995).

Oak Ridge Geomorphology, Karst and Topographic inversion

During the late Tertiary and early Quaternary periods, the portions ORR region that are currently ridge tops were at topographic foot slope and toe slope positions. These were valleys where rivers deposited alluvium. Colluvium was also deposited in these valleys from upslope positions that have since eroded. Over time, the river valleys widened. While gravel and cobble resistant to erosion and weathering collected; less resistant materials were destroyed. Eventually the river channels shifted to the sides of the gravel deposits and began to cut downward forming new valleys where the old ridges once stood, completing the topographic inversion (Figure 5). Deposits of now ancient alluviums placed before the inversion may still be found on the crest of Copper Ridge.

Karst processes helped to preserve the ancient alluviums. Water movement through cracks and joints in the dolomite and limestone of the Knox

TOPOGRAPHIC INVERSION

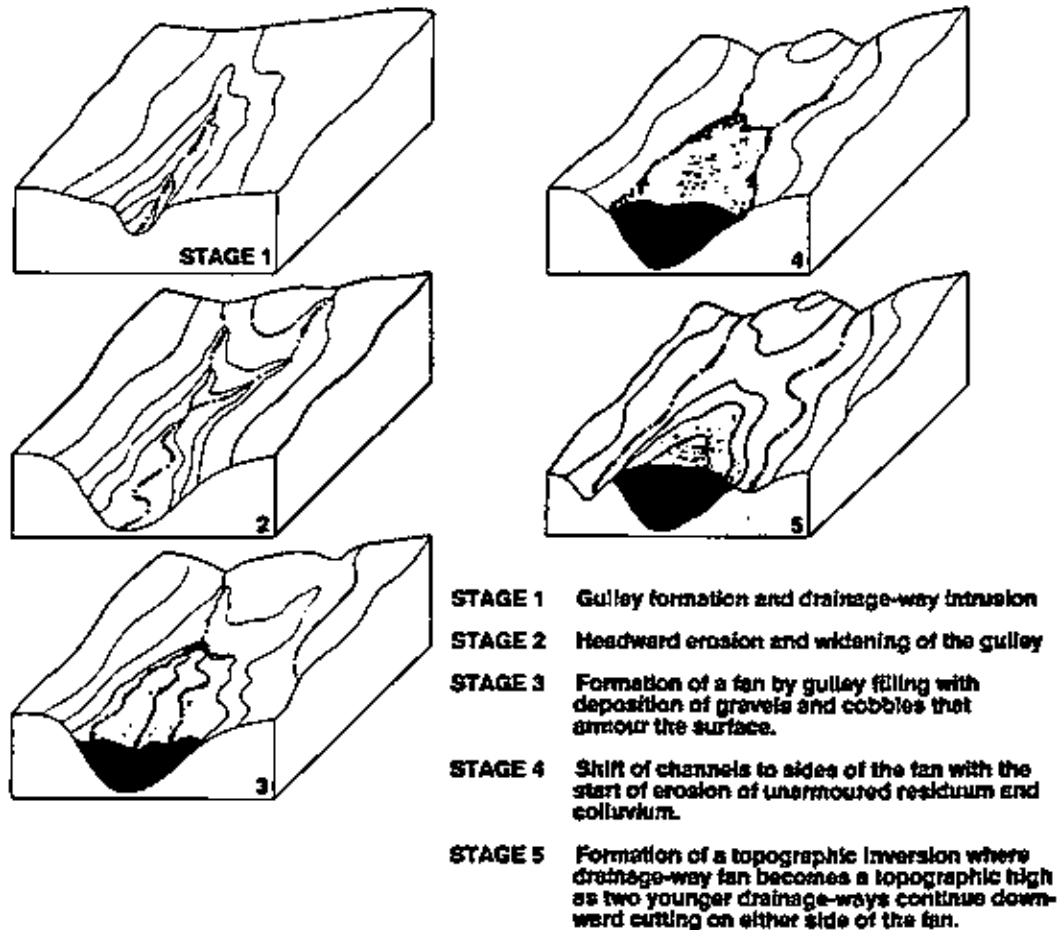


Figure 5: Topographic Inversion (from Lietzke, 1994). Old soils, some of which are alluviums, are found on the tops of ridges on the ORR due to the inversion.

group created dolines in the ORR ridges. Dolines are geomorphology defined as “a collapse structure without an open swallow hole” (Lietzke, 1994). These structures help protect pockets of ancient soil from erosion.

During the late Pleistocene, and to a lesser extent the Holocene, cycles of erosion and denudation changed the geomorphology of the ORR. These events were associated with “periods of maximum glaciation”, although the glaciers never reached that far south. During this time, much of the colluvium exposed today was created. Some of the soils were eroded down to bedrock while other more stable soils were not greatly affected (Lietzke, 1994).

The modern era (the past 300 years) has seen much of the ORR land cultivated or used as pasture. Agriculture increased erosion, created plow zones and changed the nature of the vegetation. Farming ended in 1941 when the Atomic Energy Commission took the site over (Lietzke, 1994). While the place of core extraction is currently wooded, it was probably farmed in the past.

Oak Ridge Reservation Soils

The complex geomorphic history described above has led to an intricate collage of soils on the ORR. Here I will describe soil classifications, and the factors controlling the formation of soil profiles and soil horizons as applied to the soils of the ORR. There are five factors that control the formation of soil; climate, organisms, relief, parent material and time. Soils produced under the influence of these factors are represented as profiles, each made up of two or more horizons which have a distinct set of characteristics (color, ped structure,

mineral content, roots, etc) that are used to determine a horizon designation. In a general and simplified form, horizons in a soil profile are designated as follows: the A-horizon is the upper most horizon and is influenced directly by plants and animals, the atmosphere, and the forces of erosion. Water infiltrating the A-horizon from the surface translocates material to lower horizons. The B-horizon is located below the A-horizon and receives translocated material. Characteristics of translocation (illuviation) in a B-horizon include argillans (voids filled with clay). Finally, C-horizons are unmodified horizons made up of parent material from which the soil formed. This may include saprolite (weathered rock material), and sediment packages deposited by wind or water. The occurrence and nature of these horizons, and other less common horizons not described here, allow for soil designation into one of twelve possible soil orders using the U.S. Department of Agriculture soil taxonomy system (Soil Survey Staff, 1975). There are five USDA soil orders recognized on the ORR. These are ultisols, mollisols, entisols, inceptisols and alfisols (Hatcher, 1992). Here I will briefly discuss definition of each soil order, as well as its abundance, distribution and topographic position on the ORR (Figures 6 and 7).

Ultisols, which dominate the ORR (75% by area; Figure 8) are so named because they are the ultimate product of weathering processes. These soils are defined geochemically by their base saturation level, less than 35%. Base

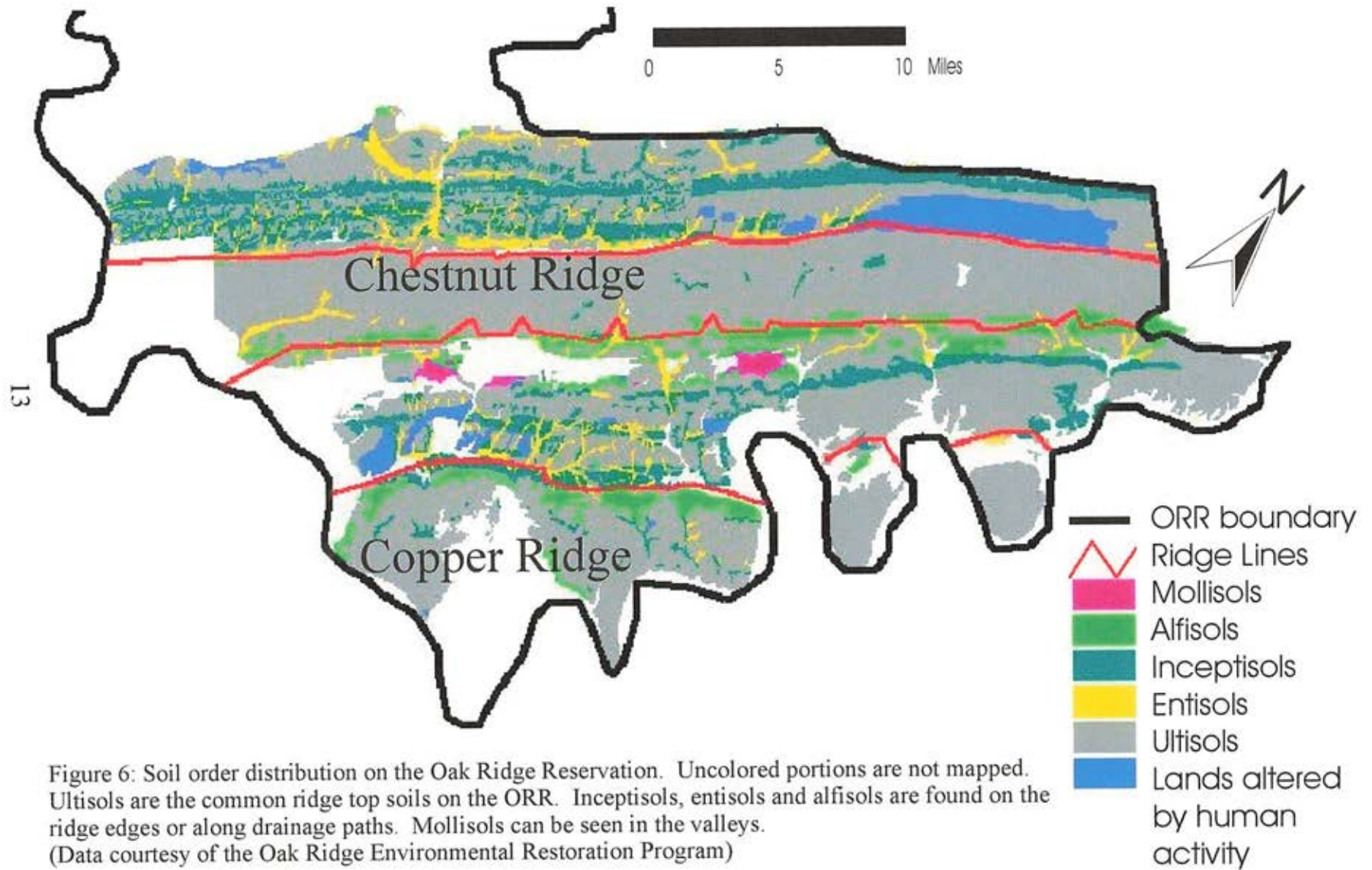


Figure 6: Soil order distribution on the Oak Ridge Reservation. Uncolored portions are not mapped. Ultisols are the common ridge top soils on the ORR. Inceptisols, entisols and alfisols are found on the ridge edges or along drainage paths. Mollisols can be seen in the valleys. (Data courtesy of the Oak Ridge Environmental Restoration Program)

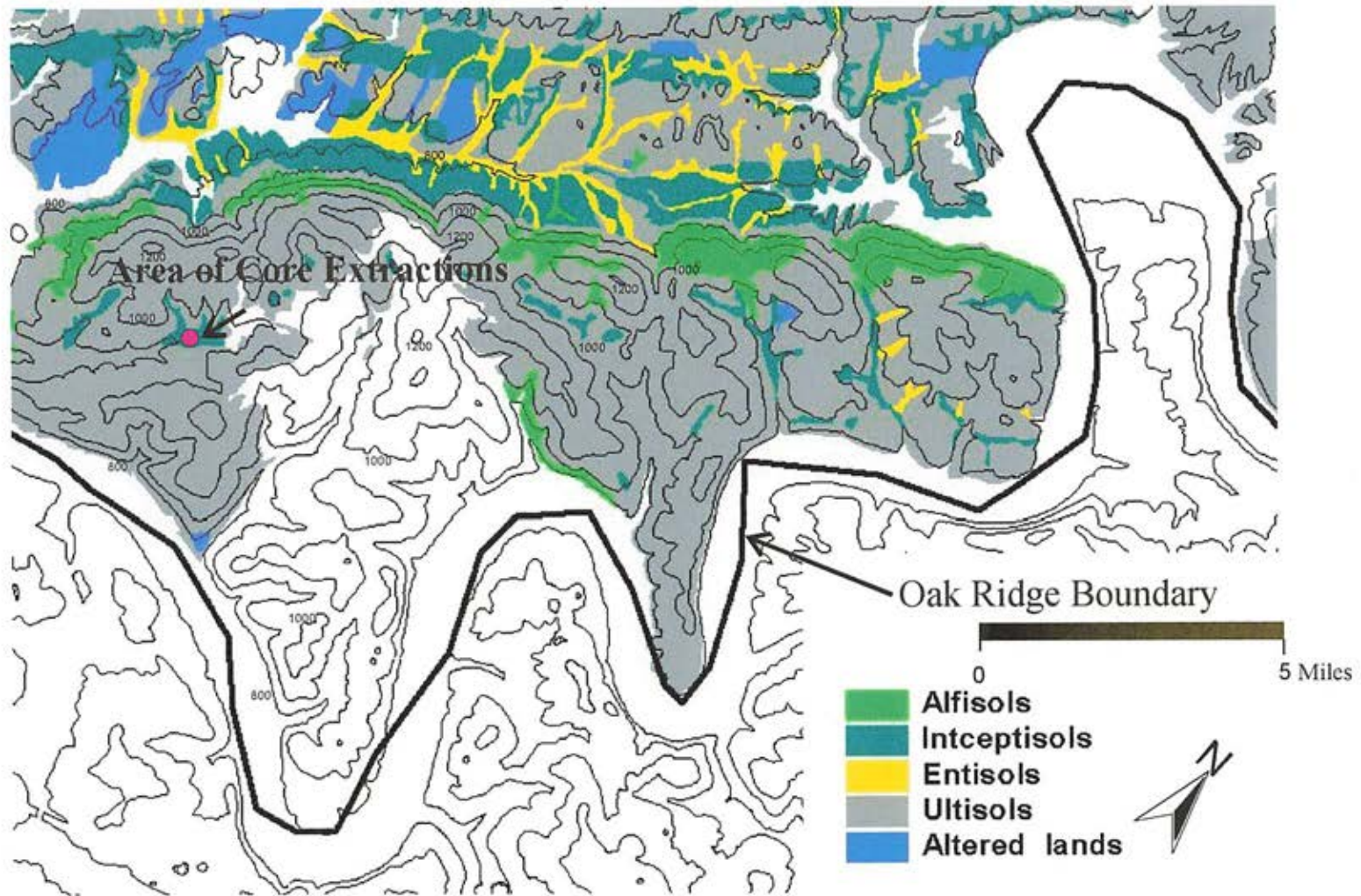
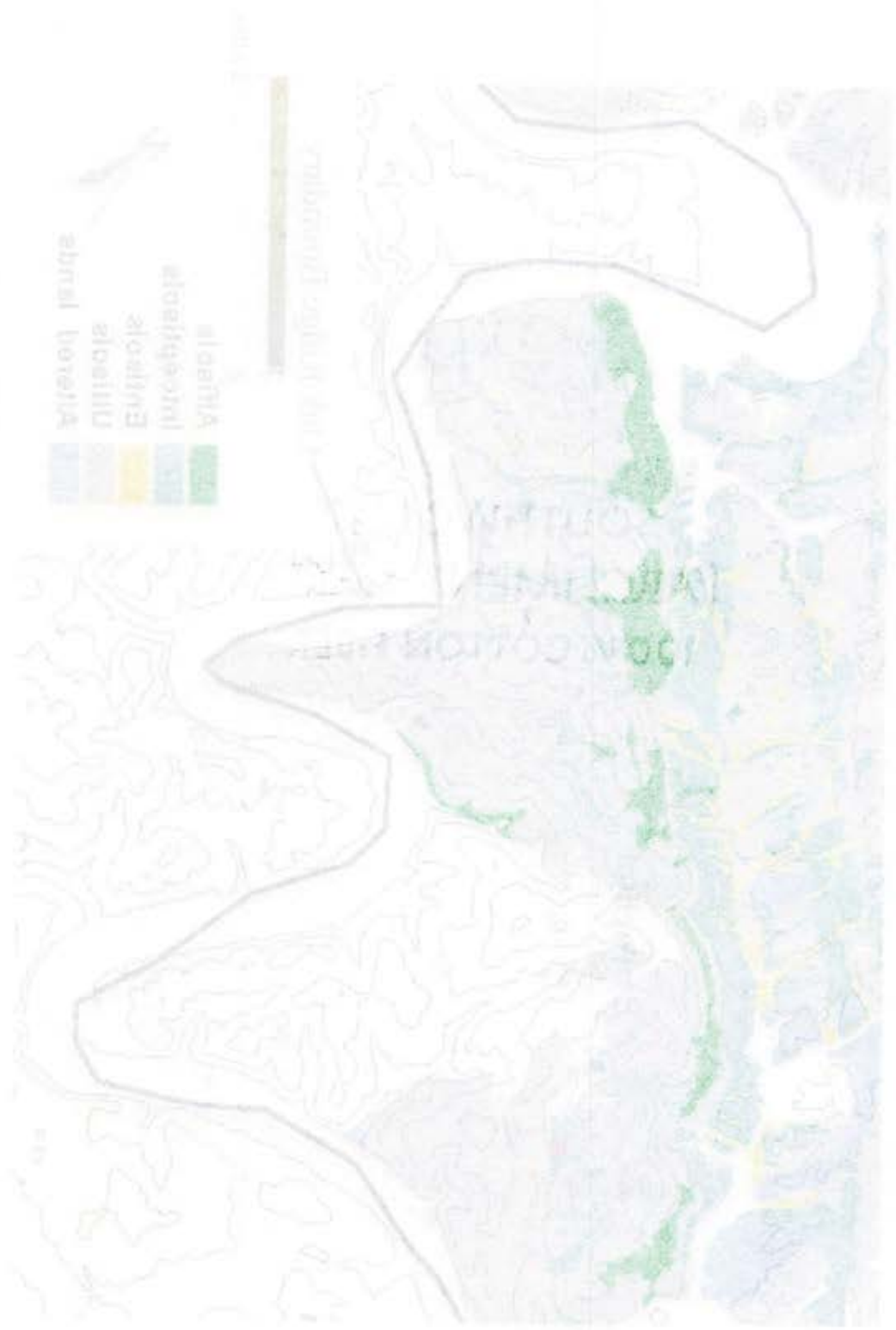


Figure 7: The distribution of soils on Copper Ridge. White areas were not mapped. Ultisols make up most of the soil on the ridge. Alfisols, inceptisols and entisols form on the less stable ridge slopes where there is less time for pedogenesis before removal by erosion, and in valleys where pedogenesis of alluvial sediments is interrupted due to burial by new sediments (data courtesy of the Oak Ridge Environmental Restoration Program)..

Figure 1. Map of the study area showing the distribution of the five species of the genus *Phyllanthus* in the region of the Rio Negro, Brazil. The map displays the distribution of *Phyllanthus* species in the region of the Rio Negro, Brazil. The legend indicates the following species: *Phyllanthus* (light blue), *Phyllanthus* (yellow), *Phyllanthus* (green), *Phyllanthus* (purple), and *Phyllanthus* (dark green). The map also shows the Rio Negro river and the surrounding topography.



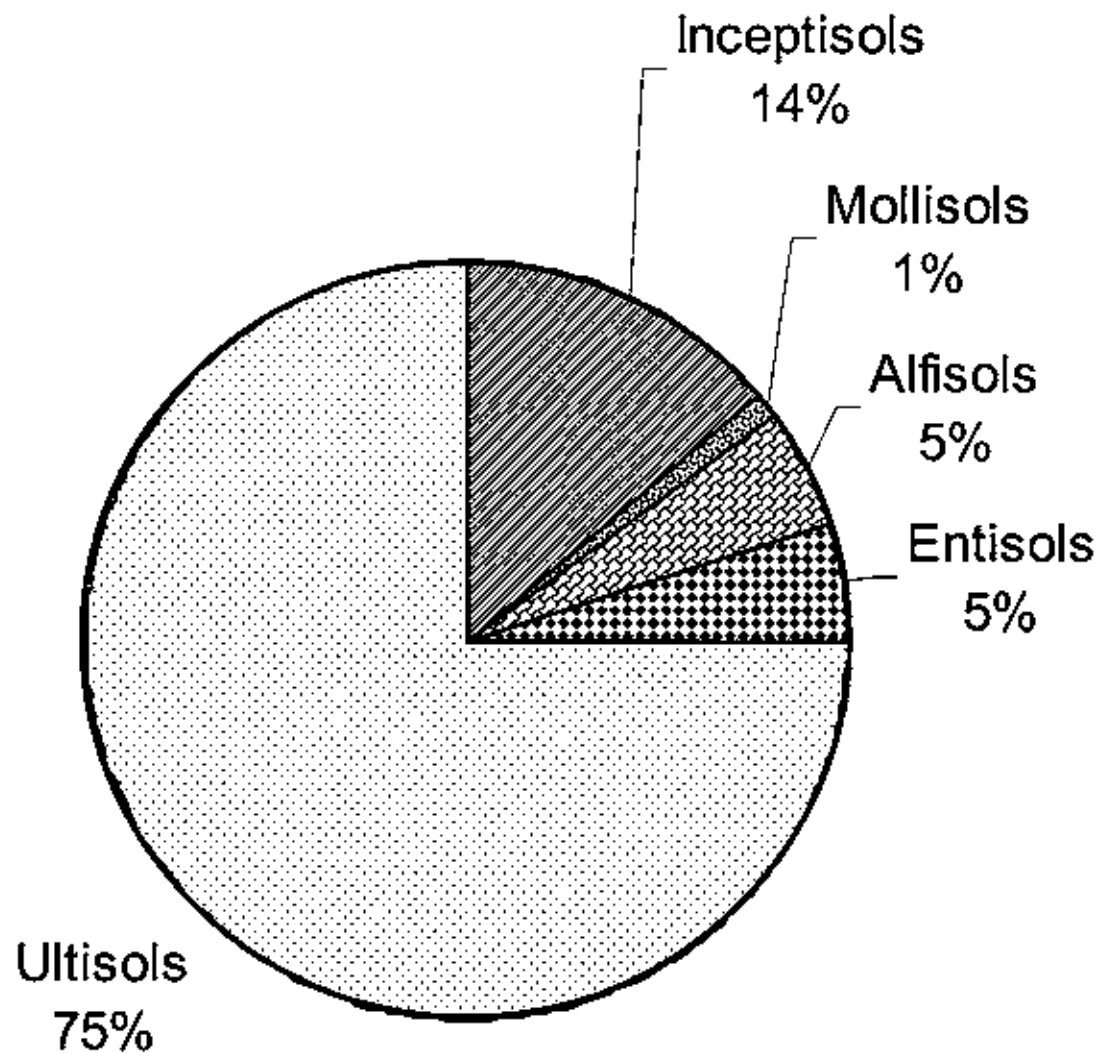


Figure 8: Percentage of soil orders on the Oak Ridge Reservation by area. Ultisols are the most common soil due to high levels of precipitation and leaching. (Data courtesy of the Oak Ridge Environmental Restoration Program).

saturation refers to the “percentage of base ions (non-hydrogen) that make up the total exchangeable cations in a soil” (Birkeland, 1999). Exchangeable cations are those attracted to the negatively charged colloids in the soil. If base saturation is low, hydrogen cations occupy the sites making the soil acidic. This happens when most of the soluble cation-donating material has been leached from the soil. Although E horizons (horizons of leached soil in the upper part of the profile) are not required for a soil to be termed an ultisol, they are common in ultisols. The leaching is a product of the movement of water through the soil profile. Bt horizons are thick (8-30 cm) and defined by a greater amount of clay relative to the horizons above and below. This horizon is created by clay translocation from horizons above and must be present to term a soil an ultisol. Production of ultisols requires a large amount of water, consequently they are most often found in humid regimes. In this region of Tennessee rainfall averages 52 in a year (Solomon et al., 1992), therefore ultisols are common.

Alfisols are much less common on the ORR, making up only 5 percent of the soils (Figure 8). Alfisols are deciduous forest soils, similar to ultisols but with a base saturation of greater than 35%. These soils are less leached than ultisols but like ultisols, show evidence of the translocation of material (often clay) from the A-horizon to a lower well-developed Bt horizon. On the ORR alfisols are situated on the shoulders of the ridges (Figures 6 and 7) where soil instability is greater than on the ridge tops. With greater instability, there is less time for the soil to be leached before it is moved downslope due to colluviation. This exposes new material, keeping the soils of this topographic position in the alfisol base

saturation range.

Down slope from the shoulder (the back slope), but running parallel to the alfisols are the inceptisols (Figures 6 and 7). Inceptisols represent incipient development of an A/Bw/C profile. These soils have less well-developed B-horizons (Bw) than the Bt horizons that define the alfisols. Bw-horizons are defined only by the absence of parent material structure and of weatherable minerals (Birkand, 1999). The less mature nature of the soils at the back slope topographic position is the result of greater instability yielding a greater rate of erosion. The erosion does not allow time for this soil to mature before being stripped away by weathering. Inceptisols are also associated with drainage patterns on the side slope of Copper Ridge. These inceptisols are created by deposition of sediments by storm flow. The soils are covered with new sediment before becoming mature enough to become ultisols.

Entisols define the least mature soil type (even less mature than inceptisols) and are evidenced by the presence of A/C profiles. These soils are too immature to have begun translocation of materials from the upper horizons to the lower horizons, and do not have a B-horizon (accumulation horizon of translocated materials). The A-horizon, therefore, lies directly on the parent material (C-horizon). These soils are associated with the local drainage pattern in the region, consisting of colluvium deposited by runoff from the ridges into the valleys (Figures 6 and 7). These sediments are deposited with such rapidity that they have no time to mature before being buried by sediments.

Lastly, mollisols, which only make up 1% of the ORR soils, are defined by the existence of a diagnostic surface horizon (mollic epipedon) which has a hue darker than 3.5 (wet) and 5.5 (dry) on the Munsell scale (Munsell Soil Color Charts, 2000). Mollisols contain greater than 0.6% organic material, and have a base saturation of greater than 50%, both of which are high relative to ultisols. The high base saturation implies less leaching of these soils than in ultisols. These are grassland soils associated most often with the Midwest. The few that are found on the ORR are in the valleys.

It is clear from the quantity of ultisols that climate (rainfall) is an important factor in soil formation here. The distribution of the non-ultisol soil is a function of topography and drainage. On Copper Ridge (Figure 7) ultisols are ubiquitous, alfisols and are found mostly on the northern edge of the ridge and inceptisols and entisols are found in valleys that drain the ridge.

Discovery of Magnetic Soils on the Oak Ridge Reservation

The paleodults or ancient alluviums on the ORR contain maghemite (Lee et al., 1984; Hatcher et al., 1992; Kopp and Lee, 1987). Evidence of their age includes highly weathered and iron-oxide-impregnated chert fragments. Clues to past alluvial influence include occasional rounded metaquartzite cobbles. These soils are found on top of Copper Ridge top as a result of topographic inversion.

The airborne geophysical data collected in 1993 showed magnetic bull's-eye anomalies, presumably due to the presence of maghemite in soil (Figures 9 and 10). Yet soil maps provided by the Oak Ridge Environmental Restoration program do not show precise correlation

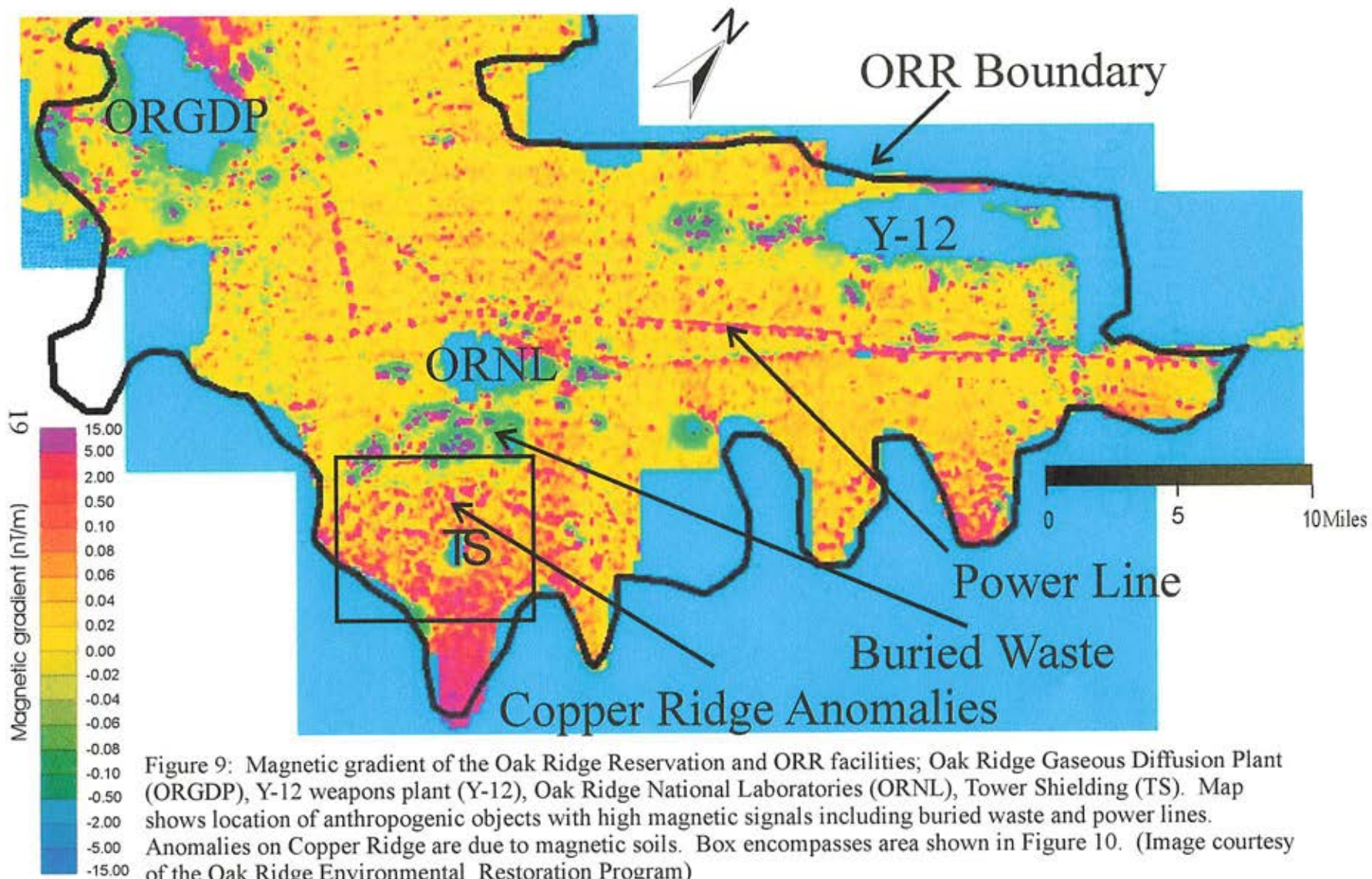


Figure 9: Magnetic gradient of the Oak Ridge Reservation and ORR facilities; Oak Ridge Gaseous Diffusion Plant (ORGDP), Y-12 weapons plant (Y-12), Oak Ridge National Laboratories (ORNL), Tower Shielding (TS). Map shows location of anthropogenic objects with high magnetic signals including buried waste and power lines. Anomalies on Copper Ridge are due to magnetic soils. Box encompasses area shown in Figure 10. (Image courtesy of the Oak Ridge Environmental Restoration Program)

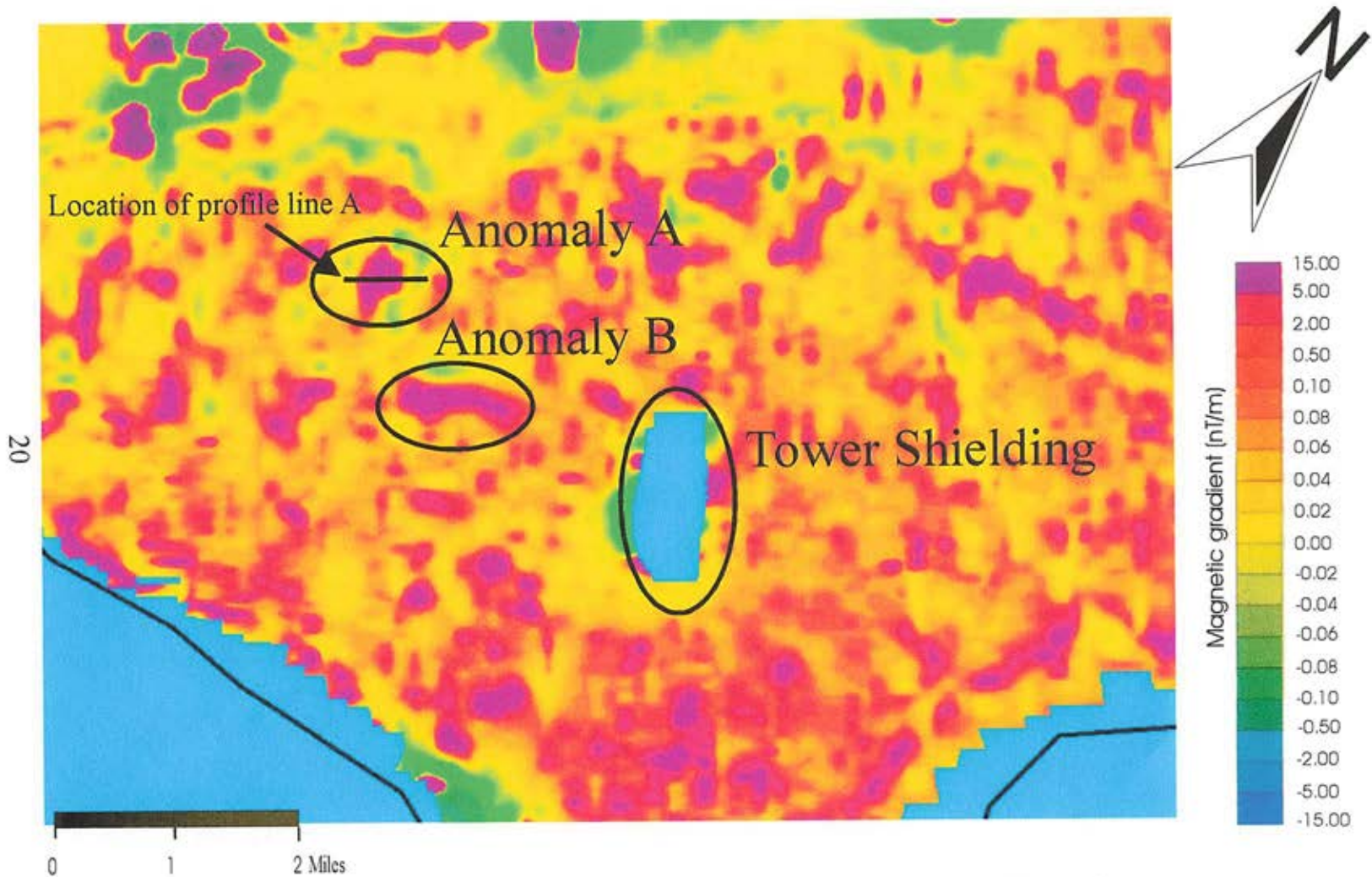


Figure 10: Magnetic Anomalies on Copper Ridge including anomaly B, which was verified by walkover magnetometry (Figure 11) and anomaly B from which the magnetic cores were extracted. (Data courtesy of the Oak Ridge Environmental Restoration Program)

between the ancient alluviums and the magnetic anomalies. Researchers tried to verify the magnetism of the soils by testing the susceptibility of the underlying rock, using walkover magnetometry to confirm anomalies discovered by the airborne survey, and measuring the susceptibility of topsoil samples and soil cores (Doll et al., 1995). Helm (1995) showed that all three groups of the ORR bedrock (Conasauga, Knox and Chickamauga) have weak magnetic susceptibilities, averaging below 50×10^{-5} S.I. The Copper Ridge Dolomite, which occurs on the ridge tops and underlies the magnetic soils, has an average magnetic susceptibility of 5×10^{-5} S.I. Using a GEM systems proton precession magnetometer, the magnetic field was measured along profile lines over the aerially mapped bull's-eyes and confirmed the anomalies including anomaly A. (Figures 10 and 11). The magnetic profile of anomaly A showed peaks 50-200 ft long, suggesting layers of magnetic material. Magnetic susceptibility of soils sampled from various anomalies further verified the presence of magnetic soils (Nyquist and Doll, 1996).

Using these data as a guide, Oak Ridge researchers collected soil cores and their magnetic susceptibilities using a Bartington MS2 meter and 80mm-diameter MS2C core sensor (Doll and Kaufmann, unpublished data) (Figures 10, 12). Their work showed that the soil in the magnetic bull's-eye (anomaly B) had a magnetic susceptibility as high as 400 (S.I. units $\times 10^{-5}$) in the upper 2 ft of the soil core. The susceptibility of the same core was greater than 100 S.I. units $\times 10^{-5}$ to a depth of more than 50 ft. A core taken outside of anomaly B showed average magnetic susceptibility of less than 20 S.I. units $\times 10^{-5}$ to a depth of 15 ft

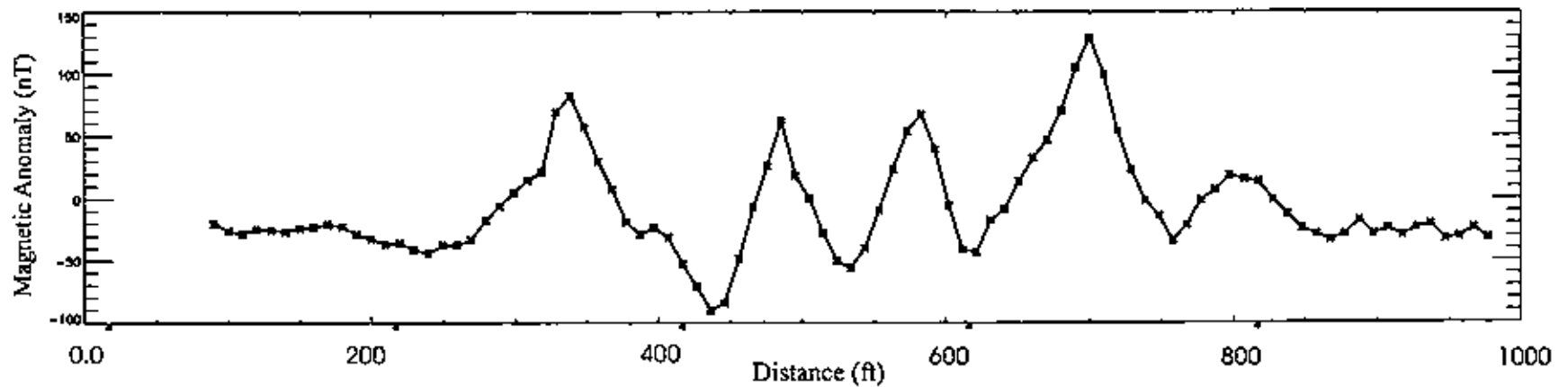


Figure 11: Magnetic profile across anomaly A. This profile confirmed the existence of a magnetic anomaly originally discovered by an airborne survey. The peaks are broad (50 to 200 feet), suggesting layers of magnetic material and not narrow peaks, as would be expected in a profile over shallow buried metal drums (Courtesy of Dr. William Doll).

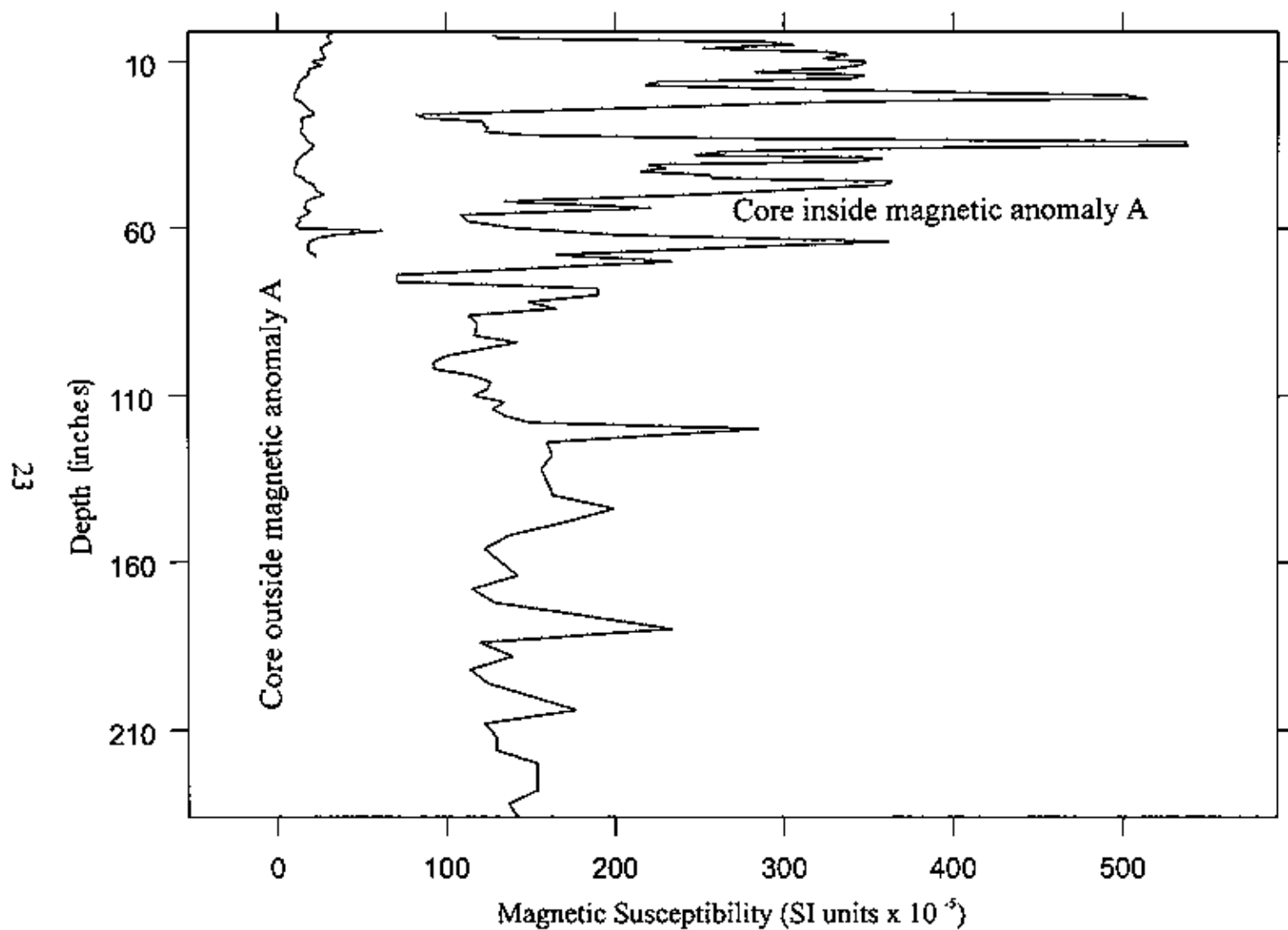


Figure 12: Magnetic susceptibility of cores on Copper Ridge. The magnetic core from inside the magnetic anomaly shows high susceptibility relative to the nonmagnetic core. (Data below 120 inches courtesy of the Oak Ridge Environment Restoration Program)

where the core terminates (Figure 12).

Doll (personal communication) did find a correlation between the magnetic anomalies and topographically lower areas of Copper Ridge, ORR (Figure 13). He suggested that karst features on the ridges influenced the position of the anomalies.

The discovery of magnetic soils on the ORR, and magnetic bull's-eye anomalies associated with them, has led to questions as to the mechanism(s) that magnetized the ORR soils. In order to understand the possible mechanisms, it is necessary to review the magnetic properties of minerals, which cause soils to be magnetic.

Magnetic Properties of Minerals

The magnetic susceptibility of the ORR soils is a product of the susceptibility of the minerals within them. The magnetic field measured at the Earth's surface is a product of the field induced by the outer core and is effected by the susceptibility of nearby material to being magnetized.

Magnetic susceptibility (k) can be calculated using the following equation:

$$B=H\mu_0 + H\mu_0k$$

where B equals the measured flux density (Tesla), H , the inducing

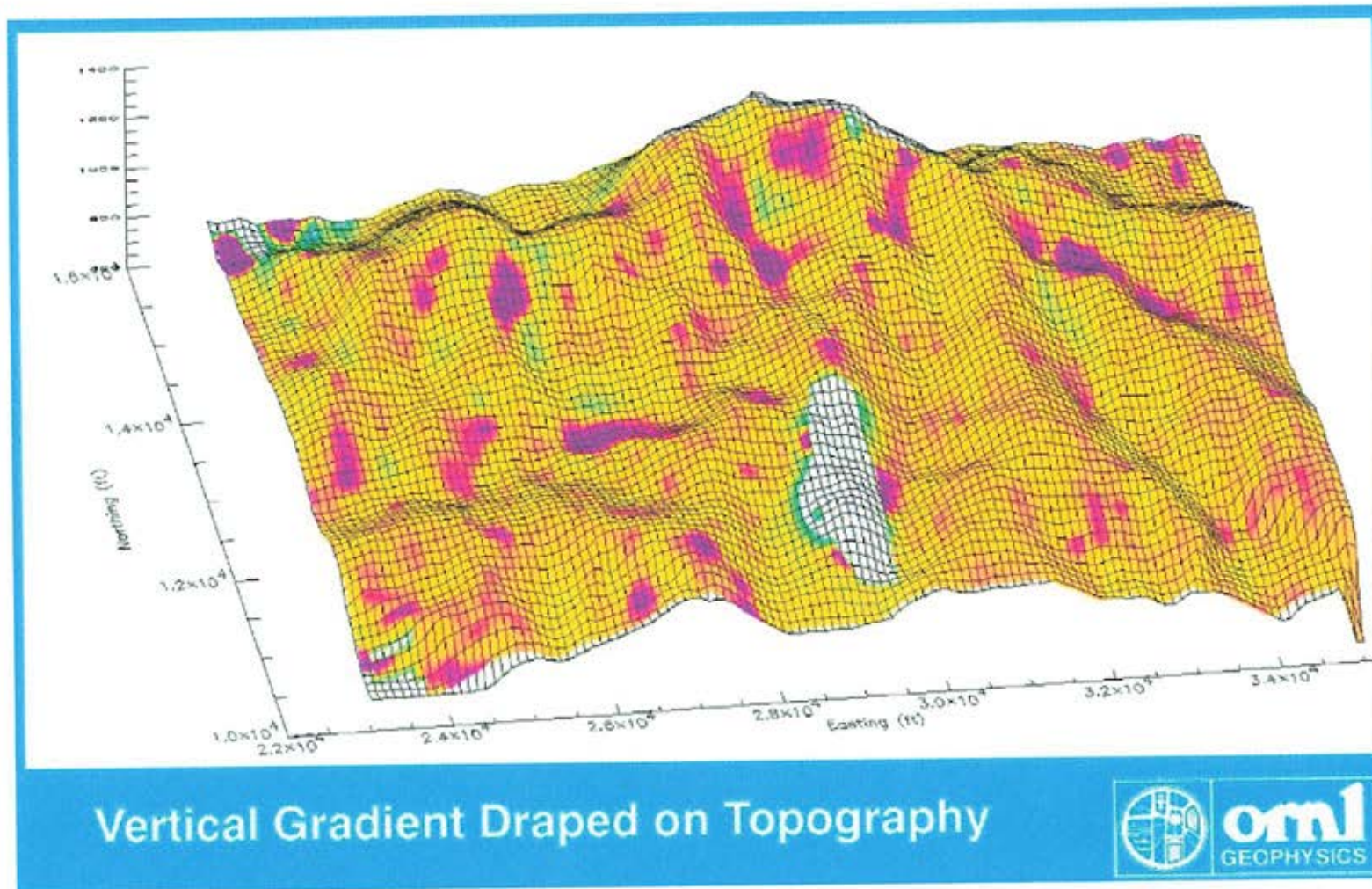


Figure 13: Magnetic gradient in relation to topography. The magnetic anomalies (magenta) are found in low lying areas on Copper Ridge. The low lying areas reflect dolines on the ridge in which magnetic soils have collected. The dolines are often oriented perpendicular and parallel to the strike of Copper Ridge indicating an association with the Copper Ridge fracture set. (Courtesy of Dr. William Doll)

field strength (Ampere/meter) and μ_0 , the magnetic permeability of free space (Weber/Amper-meter). When reporting magnetic susceptibility (which is dimensionless), rationalized SI units are used. An important property of rocks, magnetic susceptibility can be positive or negative (Halliday et al., 1997). All minerals possess magnetic susceptibility and thereby affect the measured flux density near them. The magnetic properties of minerals fall into the following classes:

DIAMAGNETISM: Diamagnetism is a magnetic property that results from the interaction of a magnetic field with the orbital motion of electrons. This causes a magnetic moment in the opposite direction of the applied magnetic field, which results in a negative susceptibility that is insignificant compared to other stronger magnetic behaviors. Examples of these usually weakly magnetic materials include quartz ($k = -1.5 \times 10^{-5}$ SI) and gypsum ($k = -1.5 \times 10^{-5}$ SI) (Tompson and Oldfield, 1986; Reynolds, 1997).

PARAMAGNETISM: Paramagnetism occurs when “individual atoms, ions or molecules possess a permanent magnetic dipole moment” (Tompson and Oldfield, 1986). These moments align themselves in a magnetic field causing a weak positive susceptibility. Without an applied magnetic field the alignment of the moments is lost due to thermal agitation. Paramagnetism tends to be stronger than diamagnetism but weaker than ferromagnetism. Pyrite (150×10^{-5} SI) is an example of a paramagnetic mineral (Dunlap and Ozdemir, 1997).

FERROMAGNETISM: Ferromagnetism is a property characterized by a change in the magnetic behavior of a material above a certain temperature called the Curie point. Because of thermal agitation, ferromagnetic materials behave as paramagnets above the Curie point. As the temperature of the ferromagnetic material falls below the Curie point, interactions occur between adjacent atomic spin magnetic moments. The atoms behave collectively as a small magnet, their collective moments referred to as magnetic domains. "For a crystal as a whole, however, the domains are so oriented that they largely (but not wholly) cancel each other as far as their external magnetic effects are concerned." (Halliday et al., 1997). The internal magnetic field of ferromagnetic material that is not canceled by the arrangement of the domains will be aligned with an external magnetic field when the material cools below the Curie point. This is called remnant magnetization. Once the Curie point is crossed the magnet is permanent, occurring without the need of an external field. If ferromagnetic material is placed in an applied field, magnetic domains oriented with the applied field will grow at the expense of other domains. Domains not oriented with the applied field will shift toward the applied field direction. These two phenomena create a strong induced moment in ferromagnetic materials. The net magnetic moment in these materials (below the Curie point) is greater than diamagnetic or paramagnetic materials (Tompson & Oldfield, 1986; Halliday et al., 1997). An example of a ferromagnetic mineral includes hematite (Fe_2O_3 ; k (approx) = 318×10^{-5} SI).

Ferrimagnetism is a variant of ferromagnetism that results in the formation of a strong internal magnetic field. Ferrimagnetic crystals contain two magnetic sites in their structure that are antiparallel and unequal, creating a net magnetic moment. This may be a function of different ionic populations on the two sites or crystallographic dissimilarities between the two sites” (Tompson & Oldfield, 1986).

Antiferromagnetism is a variant of ferromagnetism where two sites are equal in magnitude but oppose each other creating a weak magnetic moment (mutual cancellation). (Tompson and Oldfield, 1986).

The magnetic behavior of ferromagnetic minerals depends on crystal structure. Hematite and maghemite are polymorphs, minerals with the same chemical composition but with different crystal structures. Greek letters are used in their respective chemical formulas to differentiate them from one another. Hematite ($\text{Fe}_2\text{O}_3\alpha$; k (approx) = 318×10^5 SI), for example, has a hexagonal crystal structure resulting in domains oriented in such a way as to cancel their respective magnetic effects (antiferromagnetic). Maghemite ($\text{Fe}_2\text{O}_3\beta$; k (approx) = $212,000 \times 10^5$ SI) is cubic and its structure results in antiparallell magnetic domains that are unequal creating a magnetic moment (ferrimagnetic). Therefore, two minerals with the same chemistry can have very different magnetic properties (Tompson and Oldfield, 1986; Halliday et al., 1997).

Maghemite in Soils

On the ORR, maghemite forms both as glaeboles (rounded precipitates) that are referred to as “shot” (Hatcher et al., 1992), and as a replacement mineral in

chert and siltstone (Lee et al., 1984). Lee et al. (1984) suggested that the presence of maghemite in the soils was a function of “dehydration of Fe²⁺ Fe³⁺ hydroxy salt”, a mechanism suggested by Schwertmann and Taylor (1977). Magnetite includes both ferric (+3) and ferrous (+2) forms of iron. Ferric iron is associated with oxidized conditions and ferrous iron with reduced.

There have been many mechanisms of maghemite formation as a direct result of biological (microbial) as well as activity in soils abiological (Dearing et al., 1996). Magnetite can readily oxidize to maghemite (Taylor and Schwertmann, 1974), so mechanisms only involving the formation of magnetite are included below. These include:

1) *Long term weathering and pedogenesis that concentrates primary residual ferrimagnetic minerals.* Singer and Fine (1989) showed that soils formed on iron rich parent materials have a greater magnetic susceptibility than soils formed on iron-poor parent materials. This mechanism can probably be rejected for the Oak Ridge soils since the parent materials do not show high magnetic susceptibility, nor is dolostone an iron-rich parent material. The possibility should be recognized, however, that the ancient river system described by Lietzke (1994) (Figure 5) supplied iron from a distal iron rich sediment source. Singer and Fine (1989) went on to show that soils formed at a mean annual temperature of greater than 6° C and mean annual rainfall greater than 1 m were subject to greater magnetic susceptibility enhancement. Oak Ridge has a mean annual temperature of 14° C and a mean annual rainfall of 133 cm (Solomon et al., 1992).

- 2) *Accumulation of relatively coarse (>1 μm) airborne magnetic particulates mainly from pollution sources.* Evidence for this is derived from spherules produced by the combustion of fossil fuels (Tompson and Oldfield, 1986). The ORR soils are located near plants that might be a source of these particles however the depth to which the soils are magnetic and the distribution of the magnetic soils makes this mechanism unlikely.
- 3) *Strictly anaerobic bacteria that produce single domain magnetite (Fe₃O₄) grains with diameters <50nm.* In this scenario, bacteria couple the reduction of iron with the oxidation of organic compounds. The oxidation of organic compounds releases energy for use by the bacteria (respiration). Iron is an acceptor of electrons removed in the oxidation process. This mechanism allows oxidized iron bearing material to be reduced directly to magnetite. Lovley (1990) states that this method of magnetite formation in soil is as likely as the oxidization of reduced iron to magnetite. According to Dearing et al. (1996), this mechanism requires that the soil profile must be waterlogged for a period of time (>5 days per year). However, even if it were to be waterlogged, “high concentrations SFMs (secondary ferrimagnetic minerals) are not linked to such anaerobic conditions” (Dearing et al.,1996).
- 4) *Anaerobic formation of greigite (Fe₃S₄) linked to microbial reduction.* If this mechanism is invoked, a sulfur bearing parent material (organics are generally low in sulfur) must be present. At a high pH (6-12) and under reducing conditions greigite, can be produced from pyrite (FeS₂). Stanjek et al. (1994) showed greigite formed at a depth of 80 cm in a gley (reduced) soil as a result

of sulfate reduction due anaerobic respiration (Stanjek et al., 1994).

Formation of the magnetic mineral at this depth does not explain magnetism in the topsoil. Dearing et al. (1996) have the same reservations with this mechanism as they do with mechanism 3. Most importantly, X-Ray Diffractometry has shown the magnetic mineralogy on other parts of the ORR to be maghemite, not greigite

- 5) *Microaerophilic assimilatory bacteria (magnetotactic bacteria) that produce chains of single-domain magnetite magnetosomes with diameters 100-220nm.* Fassbinder et al. (1990) have located fossilized magnetic bacteria in soils. In mechanism 3 the magnetotactic bacteria are dissimilatory, transforming organic forms of elements to inorganic forms to produce energy. During this process iron is used as an electron acceptor. In mechanism five the bacteria is assimilatory, incorporating the iron into the organism's structure. Dearing et al. (1996) claim that in magnetic soils shown to contain the magnetosomes, the percentage of magnetosomes found is not great enough to explain the ferromagnetic content of the soils. Further, the size of the magnetic single-domain grains they produce is not consistent with the sizes of the magnetic grains that most often populate magnetic soils. Therefore, this mechanism is been found to be only a minor contributor to the magnetism of soils in which it has been found.
- 6) *Thermal transformation of weakly magnetic iron oxides and hydroxides to ferrimagnetic magnetite or maghemite by natural fires or crop burning in the presence of organic matter.* Magnetite can be formed during heating (fires)

that causes the reduction of iron oxides such as goethite or lepidocrocite. Oxidation occurs later during cooling, leading to maghemite. Having been cultivated or used as pastureland in the past, the area of magnetic core extraction was likely exposed to both natural and anthropogenic fires. However, Dearing et al. (1996) showed that annual fires over the course of hundreds of years do not produce strong signals in comparison to fire pits. Further, experiments by Dearing et al. (1996) showed “no significant differences after 8 years of annual burning” when compared with adjacent unburned plots. The depth and distribution of the magnetic soils on the ORR does not support this mechanism, which would result in a more ubiquitous magnetic soil distribution.

- 7) *Anaerobic microbial Fe reduction followed by formation of single-domain magnetite or maghemite ($\gamma\text{Fe}_2\text{O}_3$) grains with diameters $<100\text{nm}$.* In this mechanism common iron hydroxides such as goethite are reduced as a byproduct of microbial activity, but with no direct link to a particular organism. Later, the reduced minerals oxidize to maghemite. This is the most common source of organically influenced magnetism in soils (Mullins, 1977). The formation of maghemite is the product of redox cycles within the topsoil. (Mullins, 1977). The amount of magnetite produced is a function of iron availability and the frequency of redox cycles.
- 8) *Abiological weathering of the Fe(III) bearing minerals followed by oxidation leading to magnetite or maghemite, as demonstrated in synthetic experiments (Taylor et al., 1987).* It may not be possible to differentiate this mechanism

from the abiological mechanism above (mechanism 7). The morphology of the magnetite is the same. This mechanism is essentially the same as mechanism 7 but the redox conditions necessary to create the magnetite or maghemite are associated with abiological mechanism such as water table fluctuations.

9) *Fulgurites (formations caused by lightning strikes) may also be a mechanism for the anomalous magnetism in soils.* The powerful electromagnetic fields associated with fulgurites align domains in iron crystals to cause a strong residual (remnant) magnetization, which could generate anomalous magnetism in soils. Heat from fulgurites causes silica to melt and fuse together to create vesicular glass called dechatelierite (Giford, 1999). Glass created from the melting of silica has not been reported in soils of ORR. Although subsequent burial of fulgurite magnetized soil is possible, the depth of the magnetic signal in the ORR soils casts doubt on fulgarites as the main mechanism of soil magnetization.

Hypotheses Proposed

Some mechanisms for the formation of magnetic soils on the ORR were dismissed before testing began. Although the dolomite which underlies anomaly B may contribute some iron to the creation of the magnetic soil, the fact that the dolomite is nonmagnetic makes it an unlikely source of primary magnetite (mechanism 1). This hypothesis therefore, was not tested. Likewise, the distribution and depth of the magnetic soil makes fire (mechanism 6) an equally unlikely method. This mechanism was not tested.

Although many of these mechanisms were considered unlikely, I tested mechanisms 2, 3, 4, 5, 7, 8 and 9 by characterizing the soil in the cores extracted from the ORR to determine the redox environment in which susceptibility was the greatest, making thin sections to look for glass created by fulgurites, and examining the habit of the oxides in the soils. I used scanning and transmission electronic microscopy, X-ray diffractometry and energy dispersive X-ray analysis were used to determine if the magnetic mineral is griegite (mechanism 4) or maghemite. I compared mineral size and habit to that described in the literature for mechanisms 2, 3, 5 and 7. I hypothesize that the mechanism responsible for the creation of the magnetic soils on the ORR is anaerobic microbial Fe reduction followed by formation of single-domain magnetite or maghemite ($\gamma\text{Fe}_2\text{O}_3$) grains (mechanism 7) or abiological weathering of the Fe(III) bearing minerals followed by oxidation leading to magnetite or maghemite (mechanism 8). The soil core characterization described in the next chapter will help to determine the soil magnetization mechanism.

CHAPTER 2 SOIL CORE CHARACTERIZATION

Introduction

In 1996 Dr. William Doil and Ron Kaufmann extracted two soil cores from the ORR to investigate magnetic anomaly B, which was identified during an aerial geophysical survey (Figures 9 and 10). One soil core was taken inside anomaly B and one outside. The core was stored in two-ft plastic tubes. Using a Bartington MS2 susceptibility meter they measured the magnetic susceptibility of both cores. The soil inside the anomaly had an average susceptibility greater than 200×10^{-5} S.I. units to a depth of more than 50 ft, while the 15 foot core taken outside the anomaly had an average susceptibility less than 20×10^{-5} S.I. units. The measurements on the magnetic core exhibited greatest susceptibility in the top 3-ft. Although the overall susceptibility of the core diminished with depth, peaks of increased susceptibility were found to a depth of 10 ft (Figure 12). In this phase of the study, I identified the order and suborder of the soil in the cores using the USDA soil series classification (Soil Survey Staff, 1975), correlated soil horizon changes to susceptibility changes with depth, and characterized the pedologic differences between the two soils in order to explain the occurrence of maghemite in the magnetic soil.

Both the magnetic and nonmagnetic soil cores are characterized by many episodes of deposition and pedogenesis. Colluvial material buried soils, creating a stratigraphy within the core. I have identified each soil as a distinct profile with a number. Profile 1 is the present day soil, Profile 2 is the first buried soil, Profile 3 is the second buried soil, etc. Descriptions of each profile are in Appendix 1. Schematic representation of the soil cores with pictures and susceptibility measurements are found in Appendix 2.

Procedure

Photographs were taken to document each core before study. A portion of the casing was removed from each two-ft core tube to expose the soil. With Dr. Jon Nyquist, I photographed each core using a Sony DSC755 digital camera. We took pictures of the whole core and of 5 inch sections of the core. Finally, close-up pictures were taken of specific features of interest in each core section. Each picture was numbered and documented (Figure 14). Before further work began on the photographed core, the pictures were downloaded and inspected.

After the photographs were found to be satisfactory, I documented core descriptions on a template (Figures 14). The nature of the core (magnetic or nonmagnetic), the core section depth, and the date of the description were recorded. I made representative drawings of the core to show ped structure, horizon changes, thin section sample areas, and areas from which TEM, SEM and XRD samples were taken. Magnetic susceptibility measurements were made using a Bartington MS2 susceptibility meter and were documented next to

individual cores (Figure 14, Part 1). Horizon intervals were designated and horizons briefly described and documented (Figure 14, Part 2). I then made a detailed description of each previously defined horizon (Figure 14, Part 3) including Munsell color values (wet and dry) (Munsell Soil Color Charts, 2000), mineralogy, roots, ped structure, boundary characteristics, and any additional observations prior to making thin sections.

Thin Section Preparation

I selected soil for thin sectioning based on the nature of the horizon changes (if there were any) and the magnetic susceptibility data. If abrupt changes were seen in the susceptibility and in soil characteristic with depth, material was removed for thin sectioning. For example, in Profile 6 of the magnetic core, at a depth of 62 inches, an increase in soil competence, a decrease in chert content by 60%, and a change in ped structure from blocky to columnar represents an abrupt change in soil characteristics. These characteristics persist to a depth of 68 inches. A thin section was selected in this interval at a depth of 64 inches where a magnetic susceptibility peak occurs.

Once a section of the core had been selected for thin sectioning, a 1-2 in portion of that section was removed. In cases where the soil was cohesive, I removed a cylindrical slice of the core and documented "up" by marking arrows on the soil. In cases where the soil was not cohesive, peds were removed from the core. Up direction was marked on the ped, but in some cases the soil was disturbed upon the removal of the core casing and the up direction may not have been accurate.

Core Section _____ Date _____

| <u>INCHES</u> | <u>MAG READING</u> (uncorrected) | <u>CORE</u> | <u>SAMPLES TAKEN</u> |
|-----------------|-------------------------------------|-------------|--------------------------------------|
| Stopped 48 0 | | start here | |
| 49 1 | | | |
| 50 2 | <u>929</u> | H1 | |
| 51 3 | | | |
| 52 4 | <u>236</u> | H2 | 75YRW80, |
| 53 5 | | | |
| 54 6 | <u>388</u> | | |
| 55 7 | | | |
| 56 8 | <u>191</u> | H3 | |
| 57 9 | | | |
| 58 10 | <u>199</u> | | more chert Thin Sect 01 assess |
| 59 11 | | | |
| 60 12 | <u>248</u> | H4 | TEM Mag 8201 |
| 61 13 | | | |
| 62 14 | <u>349</u> | | TEM Mag 8202 Thin Sect 02 |
| 63 15 | | | |
| 64 16 | <u>635</u> | | Thin Sect 03 |
| 65 17 | | H5 | |
| 66 18 | <u>456</u> | | |
| 67 19 | | | |
| 68 20 | <u>290</u> | | |
| 69 21 | | | |
| 70 22 | <u>410</u> | H6 | less chert |
| 71 23 | | | |
| 72 24 | | | |

Figure 14: Example soil core description, Part 1

| HORIZON & INTERVAL (cm) | DESCRIPTION | NOTES (Pics) |
|-------------------------|------------------------------------------------------------------------|---------------------------------------------------------------------|
| H ₁ 0-3 | Little chest Col. ped well consolidated | 1) Whole column (w lid) 2) " " (no lid) 3) 1/2 column 4) " |
| H ₂ 3-6 | Large amount chest blocky ped poorly consolidated root branch | 5) 1-5 6) 5-10 7) 10-15 8) 15-20 9) 20-25 |
| H ₃ 6-8 | Little chest col ped well consolidated | |
| H ₄ 8-14 | lots of chest blocky ped found small root gradual to ↓ | |
| H ₅ 14-21 | Not much chest good col ped | |
| H ₆ 21-24 | High chest | |

Figure 14: Example soil core description, Part 2

Core Section May 82
Horizon # & interval H₁

Color 7.5YR 6/6D 10YR 3/6 w
Texture and
consistence Some clay but more silt and even
some sand 35/65/10 firm
C St Sd

Mineralogy Found 1 nonmagnetic concentration (Manganese?)
in inclusions and 1 piece vermicular nodules (both in
May H₁ 8202, 102 SS piece that is angular also in May H₁ 8202
of FeO coated chert also in May H₁ 8202 (<20%)
Roots None found

Peds Columnar ...
(Size/Shape) 3 ribs, lower two fine angular, powder
under further breaking but columnar before disintegration

Other
Structures/Features/Organisms none

HCL reaction —

Boundary Sharp to H₂

Notes Found (cobble?) red in center, 1 blk on rim.
Made of sherrings, in base scratched (R). Blank
part in magnetic
Well consolidated

Figure 14: Example soil core description, Part 3

The removed portion of the core was then completely coated in Hillquist thin section C and D epoxy. I placed the coated material in a glass case from which ran tubing to a Dayton 6K778B belt drive fan and blower motor. The motor was used to create a vacuum in the casing, drawing air out of the soil and through the epoxy creating a vacuum inside of the coated soil. I maintained the vacuum for 2 minutes. I then opened a shunt allowing air to pass into the glass casing to equalize the pressure. The epoxy was drawn into the soil as the pressure equalized. I applied this process, termed vacuum impregnation, twice to each soil sample. The epoxy hardened after 24 hours, and I cut the epoxy impregnated soil into sections. The fresh (unimpregnated) surfaces were coated in epoxy and vacuum impregnated again. After this new epoxy hardened, the flat (cut) surfaces were polished on the lap wheel until the epoxy coating was removed and the cemented soil surface was reached. I then used A and B Hillquist epoxy to mount the soil on a frosted glass slide, polished side down, and allowed the sample (termed a billet) to set. After setting, the top of the billet was cut off creating a thin section. I attempted to grind the thin section down to 30 μ m. In some cases the thin section was too fragile to grind to 30 μ m and so was left 40-60 μ m thick. At no point in this process did I use water. All cutting and grinding was done dry as I found that water would be absorbed by the soil, causing it to expand and wash from the glass slide.

I analyzed the thin sections using a Nikon Eclipse E600 polarizing petrographic microscope. Using plane polarized, cross polarized, and reflected

light, descriptions of the soil matrix texture and mineralogy, root structure, ped structure, general mineralogy and other features were made. Descriptions included information on particle size, particle coatings, clay infills and chert matrix. A total of 25 thin sections were prepared for analysis which is about one thinsection for every eight inches of soil core.

Thin Section Analysis

The thin sections I made from both the magnetic and nonmagnetic core were characterized by a clay matrix with iron and manganese glaebules, chert fragments and quartz grains. The matrix was red-brown to yellow-brown (the nonmagnetic soil was more yellow and the magnetic soil was more red) clay with 20-100 μm quartz fragments through out. The clay matrix from the magnetic core had rounded mottles and glaebules from 20 μm to 2 mm in diameter (Plate 1, Picture 1). Glaebules were less common in the nonmagnetic core matrix (Plate 1, Picture 2). This was a major difference between the two cores in thin section. In both cores the clay was most often randomly oriented. In some cases however, a vosepic clay fabric (Plate 1, Picture 3) could be seen in which clay grains were aligned in voids. This fabric manifests itself in wavy optical extinction of the clay grains. Aligned clay and silt-filled linear, sub-linear and rounded voids left by the decay of organic matter or the dissolution of soluble minerals suggests translocation of material from an upper (A) horizon to a lower horizon in the soil, a common pedogenic process. Translocated clay and silt are referred to as argillans and siltans, respectively (Plate 1, Picture 3 and 4). Argillans and siltans

found in Profile 2, A-horizon suggest translocation into the first buried A-horizon from Profile 1, above. If material was translocated into Profile 2 from Profile 1, the term "overprinting" is used. Overprinting, which occurs when the properties of a buried soil are influenced by the soil above, may disguise original features in a buried soil and make classification of the soil difficult.

One major exception to the presence of a clay matrix was found in Profile 1 of the magnetic soil. The matrix in this profile was particularly rich in silt (>50%). This may be evidence of a different parent material, possibly loess.

Rounded or angular quartz was commonly found in the magnetic core thin sections in sizes ranging from 1 mm to 2 cm. Quartz in the non-magnetic soil thin sections was generally smaller (1-5 mm) and angular. The quartz grains in the magnetic core were commonly rounded or angular (subhedral). Those in the non-magnetic core were angular. A quartzite cobble, probably from a metaquartzite rock, was found in the magnetic core (Plate 1, Picture 5) and is evidence of a non-dolomite parent source. Plate 1, Picture 5 also shows iron oxide infiltration of the quartzite, a common feature in grains from the magnetic soil.

Chert was found in both soils but in different forms, including oolitic, massive and porous. Commonly the chert was partially replaced by iron oxides (Plate 2, Pictures 1 and 2). Generally, the magnetic core was rich in chert (20-60% as estimated by visual inspection of the core) compared to the nonmagnetic core (5-25%). The chert is probably relict from the underlying dolomite as it weathered away, leaving the resistant chert behind.

With the data gathered by photographing and describing the cores macroscopically and microscopically, I will characterize each by classifying the soil order and suborder using USDA soil taxonomy and proposing a possible genesis for the soil in the cores.

Characterization of the Soil Core Taken Inside Magnetic Anomaly B

Horizon Designation and Soil Classification

Soil classification can offer insight into how a particular soil formed. Before using soil core and thin section analysis to classify the soil inside anomaly B, I will detail how the horizons in the core were designated, as horizon designation will allow for proper classification. The characteristics of the soil extracted from inside anomaly B are summarized in Table 1. Generally, A-horizons in the magnetic core profiles differ from B and C-horizons by a 10-60% increase in chert content (often kaolinized), a decrease in soil competence (soil consolidation), the appearance of a blocky ped structure, and the presence of roots. Pieces of grass stems and roots were observed in three of the highest four buried A-horizons (Appendix 1 and 2; Plate 2, Picture 3).

| | |
|---------------------|-----------------------------------------------------|
| Soil Classification | Aquept |
| Location | Copper Ridge, middle of magnetic anomaly (Figure10) |
| Geomorphic Position | Center of a breached doline |
| Slope | 1-2% |
| Parent Materials | Loess and slopewash |
| Vegetation | Grasses |
| Described by | J. Rivers |
| Date | 2-18-2002 |

Table 1: Properties of the soil core inside the magnetic anomaly

It was difficult to characterize the sub-A-horizons in the magnetic core. B-horizons "show little or no evidence of original sediment or rock structure" due to pedogenesis (Birkeland, 1999). B-horizons which show only the beginning of pedogenesis are termed cambic (Bw) horizons. C-horizons are horizons unmodified by pedogenesis and which represent original parent material. Over time, C-horizons will transform to Bw-horizons as pedogenesis proceeds.

Determining whether modification of original parent material has occurred is often complicated. The parent material of this soil is colluvial material from older soils that washed into a doline from higher elevations on Copper Ridge. With the exception of Profile 1, I observed evidence of translocation (argillans and siltans) throughout the core (Plate 1, Picture 3 and 4). This suggests overprinting from overlying profiles. The nature of the parent material and the

evidence of overprinting makes it impossible to determine when the translocation occurred. This uncertainty has led me to designation sub-A-horizons as C→Bw-horizons to show C-horizons that are converting to Bw-horizons. This is referred to as soil welding (Ruhe and Olson, 1980). The C→Bw-horizons differ from A-horizons by an increase in soil competence, a decrease in chert content by 10-60%, a decrease in roots, and often by the appearance of columnar ped structure (although the A-horizon in Profile 2 displays this structure) (Appendices 1 and 2).

The horizon designation described above allows for the classification of this soil as an inceptisol. Inceptisols are soils in which the parent material has just begun pedogenic modification. These soils are normally recognized by an A/Bw/C horizon pattern. The simple A/C→Bw pattern in the soil suggests that the soil in this position had little time to begin modification of parent material before being buried by new colluvial sediment from runoff or alluvial sediment from stream flow. Modification has begun, however, as evidenced by the vosepic clay fabric (Plate 1, Photo 3), which shows clay grains of similar orientation filling a void. The designation as an inceptisol is in agreement with the soil maps provided by the Oak Ridge Restoration Project (Figure 7). Iron stains (mottles) and iron oxides, some magnetic, were found throughout each profile and in every horizon in the form of mm-size nodules, chert coatings, and clay coatings. The presence of the mottles suggests hydromorphism (Birkeland, 1999). Because I can state with certainty that the soil has been subjected to long periods of wetness, the aquic (prefix aqu) suborder has been used. This suborder applies to soils produced in such wet conditions. Therefore the soil is an aquept.

A complete particle size classification might show evidence of clay translocation within respective profiles. Dr. Yul Roh of the Oak Ridge Environmental Science Division and I attempted to separate the different size fractions of soil samples taken for SEM characterization (See the SEM section in chapter 3). The silt and clay aggregated, even after sonication, so the particle size classification is incomplete. Due to lack of time and funding, no lab analysis for base saturation was performed. Without this analysis, I cannot state with certainty that the soil is within a particular base saturation range. With the complication of older soil being the parent material and of overprinting, comprehensive particle size classification and base saturation would be helpful in classifying this soil. The above classification was made in spite of these problems.

Soil Genesis

Having designated the soil horizons and classified the soil as an aquept, it is now possible to discuss some of the mechanisms that lead to the generation of this soil. The repeated A/Bw profiles are strong evidence of a colluvial or alluvial (stream deposited) parent material. Other evidence for this is found in the soil itself. Precipitation is one of the driving forces of pedogenesis. The ORR receives 52 in. of rain per year (Solomon et al., 1992) and periodic water logging can occur in some places. Over 50 ft of core was extracted from inside the anomaly, but I only characterized the top 12 ft. At the time the core was extracted, the water table was 6 ft below the bottom of the core section I describe here (the water table was reached at 18 ft). Though the soil formed in a depression (a

doline), it is located in a regional topographic high (Copper Ridge) and would appear to be well drained.

Keeping the current water table level in mind, evidence of colluviation includes iron oxide coated chert fragments that were located in Profile 1 (Plate 2, Picture 1 and 2). The chert is coated on the outside and on void surfaces. Coatings on and within the chert suggests a fluctuating water table and possibly long periods of time. The chert is kaolinizing (breaking down into clay). Sedimentary chert is made of SiO_2 , (as opposed to igneous chert which may be feldspathic), which is very stable at the Earth's surface. The breakdown of SiO_2 is also evidence of an extensive weathering. These characteristics suggest that the chert in Profile 1, A-horizon previously occupied a position closer to the water table where it weathered for a long time. In a depression it is unlikely that erosion has exposed a previously buried horizon. It is more reasonable to assume that this material was once in a lower pedologic position closer to the water table. The chert was transported to its current A-horizon position by colluviation.

These observations concur with soil maps provided by the Oak Ridge Restoration Project and with Hatcher (1992), which show the soils in this area to be formed from sediments transported from ancient alluviums on the higher areas of Copper Ridge. Further support for an alluvial origin of the parent material was located in Profile 2, C→B-horizon where a quartzite cobble was found in thin section (Plate 1, Photo 5). The underlying dolomite is an unlikely source for such a lithology, and Hatcher (1992) states that the ancient alluviums contain "rounded metaquartzite river cobbles."

Other processes have influenced the soil in this core. An increased amount of chert in the bulk soil of Profile 2, A-horizon in comparison to the Profile 2 C→ Bw-horizon (Table 3) is probably the result of soil deflation. With deflation, silt and clay particles are removed from the topsoil by wind and runoff leaving larger particles behind. Runoff from additional major storm events then wash a new package of colluvial or alluvial material over the older deflated A-horizon. Increased amounts of chert in other buried A-horizons reflect the same process.

Finally, Profile 1, A-horizon is very silt-rich and contains a small amount of chert. I interpret this as an eolian influence as eolian soils are often silt rich (Birkeland, 1999). The reason Profile 1 has eolian parent material and the buried profiles show evidence of deflation is unclear. Perhaps the uppermost profile has yet to be deflated or perhaps there is unrecognized buried loess in the soil profile. Because of the grass fragments in the upper-most part of the chert-rich horizons, I am confident that my designation of buried A-horizons is correct. With the history of this soil in mind, it is now possible to analyze the magnetic data.

Magnetic Susceptibility of Soil

The average susceptibility of the soil inside anomaly B was 251×10^{-5} S.I. units. Susceptibility spikes are found in the core near the A/C→ Bw boundary in Profiles 1, 2, 4, 5, 6, and 7 (Appendix 2). Figure 17 shows the attributes of a typical 2-foot core section where magnetic susceptibility peaks at the A/ C→ Bw boundaries. This reflects an oxidation-reduction cycle in which maghemite is produced. During rainstorms (which may last weeks in this part of Tennessee),

the A-horizon is waterlogged (reduced) by interflow (water running through the soil). After such a storm, the A-horizon dries (oxidizes) while the C→ B-horizon remains waterlogged for a longer period. This redox boundary is the optimal environment to promote maghemite crystallization. The process only occurs in the modern soil where the atmosphere can oxidize the A-horizon but peaks in the buried profiles mark this relict redox boundary.

There is some uncertainty as to where the actual susceptibility peaks within the core. The A-horizons are less dense than the C→ Bw-horizons. The susceptibility was measured using volume susceptibility measurements before the casing was removed. If the A-horizon susceptibility measurements on my cores were mass-normalized measurements, it is possible that we would see peaks higher in the profile. Singer and Fine (1989) measured mass-normalized susceptibility with depth in 27 soils in California and found that in most cases eluvial horizons (horizons from which material has been removed) had greater magnetic susceptibility than illuvial horizons (in which material accumulated). Profile 3 shows a magnetic spike in the lower C→ Bw-horizon at a depth of 32 inches and Profile 4 shows a spike in the upper portion of the A-horizon at a depth of 36 inches (Appendix 2). The reason for the position of the Profile 3 spike is unknown. Profile 4 has an over-thickened A-horizon suggesting a cumulic nature to this profile. A cumulic soil is one in which a "soil receives influxes of parent material while soil formation is going on" (Birkeland, 1999). The addition of small amounts of sediment to the top of the soil thickens the A-horizon and

Magnetic Core 082 (#3)

Horizon Color Profile Picture

Legend

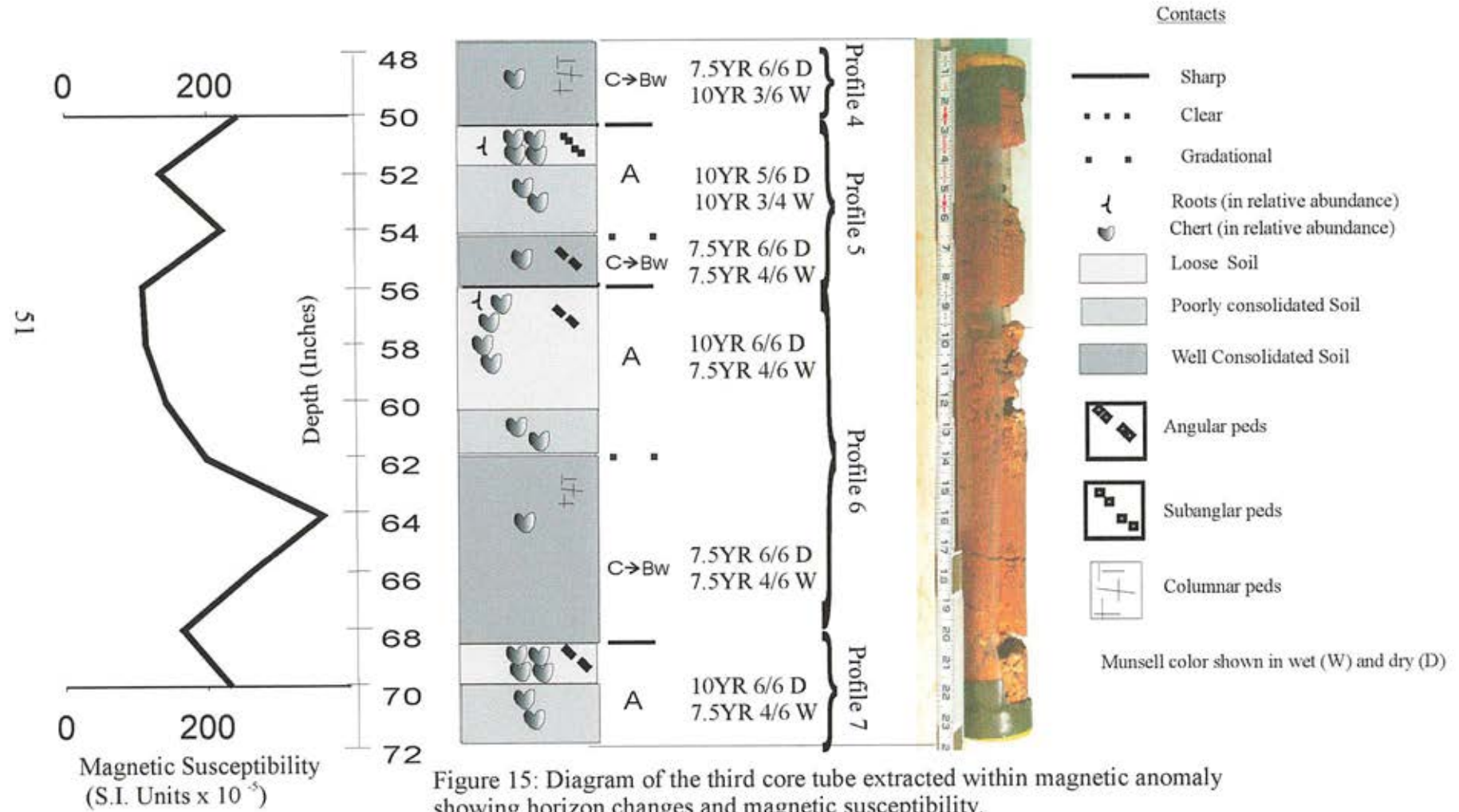


Figure 15: Diagram of the third core tube extracted within magnetic anomaly showing horizon changes and magnetic susceptibility.

changes the redox boundary (distance to atmospheric oxygen) where maghemite is formed, shifting it upward in the soil profile.

Summary

The soil recovered on the ORR from inside anomaly B is an aqucept and is a product of colluvium or alluvium washed down from the top of Copper Ridge. The parent material of the soil was derived from extremely weathered soils. The soil in anomaly B shows evidence of A-horizon deflation, accompanied by increasing chert content and weakening of horizon competence. The soil shows strong evidence of hydromorphy and so and an aquic suborder is designated. The soil is rich in iron oxide and has an average susceptibility of 251×10^{-5} S.I. Susceptibility peaks in the soil are found associated with A/C → Bw boundaries. In the next section I will discuss how the soil outside of the anomaly differs for the soil inside the anomaly.

Characterization of the Soil Core from Outside Magnetic Anomaly B

As with the soil inside anomaly B, horizon designation will allow for proper USDA soil classification. Once the soil is classified I will discuss the material and mechanisms which generated the soil.

Horizon Designation and Soil Classification

Horizon designation in the nonmagnetic core is similar to that of the magnetic core. A-horizons are defined by a marked increase in chert content

(much of which was kaolinized) and a decrease in soil competence (decrease in consolidation). Roots confirming the placement of the A-horizon were found in every profile but Profile 2 (Appendices 1 and 2). The characteristics of the soil extracted from outside anomaly B are located in Table 2.

The C→Bw is again used to describe the sub-A-horizons. The C→Bw horizons were marked by an increase in soil competence, a decrease in chert content, and by the appearance of a platy ped structure (Appendix 1 and 2). Thin sections showed the first B-horizon (Profile 1) to contain translocated clay (argillans) which cannot be a function of overprinting as this is the uppermost profile. All horizons have a mottled appearance but lack the ubiquitous iron oxide coatings and glaucules found in the magnetic soil. The translocated clay is evidence that pedogenesis has begun. The platy ped structure is probably the manifestation of relict bedding, an original deposition fabric. Original depositional fabric implies that the pedogenesis is not far advanced. Horizons into which material is being translocated but that show only the beginning of parent material alteration are termed cambic horizons and are designated Bw. Soils characterized by cambic horizons are inceptisols. The mottled appearance of the soil is evidence of hydromorphism. I therefore term this soil an aquept.

Soil Genesis

The parent material of this soil, as with the magnetic soil, eroded from old soils up slope. The increased chert content in the A-horizons is a product of soil deflation as explained previously. The presence of kaolinized chert in the nonmagnetic soil suggests that the parent material of this soil is old since the

| | |
|---------------------|-------------------------------------------------------|
| Soil Classification | Aquept |
| Location | Copper Ridge, outside of magnetic anomaly (Figure 10) |
| Geomorphic Position | Edge of a breached doline |
| Slope | 1-2% |
| Parent Materials | Locss and slopewash |
| Vegetation | Grasses |
| Described by | J. Rivers |
| Date | 2-18-2002 |

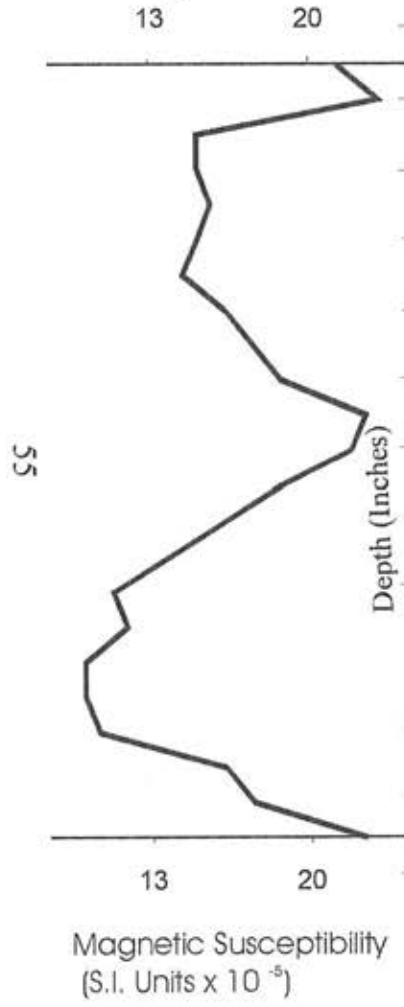
Table 2: Properties of the soil core outside the magnetic anomaly

breaking down of chert to clay is a slow process, possibly on the order of thousands of years or more. The original deposition features (platy ped structure) observed in the soil suggest a relatively young soil, and it is unlikely that the chert kaolinized in place. Thin sections revealed a smaller number of iron glaeboles when compared to the magnetic soil source (Plate 1, Pictures 1 and 2). It is probable that the iron content effects the magnetic susceptibility of the soil.

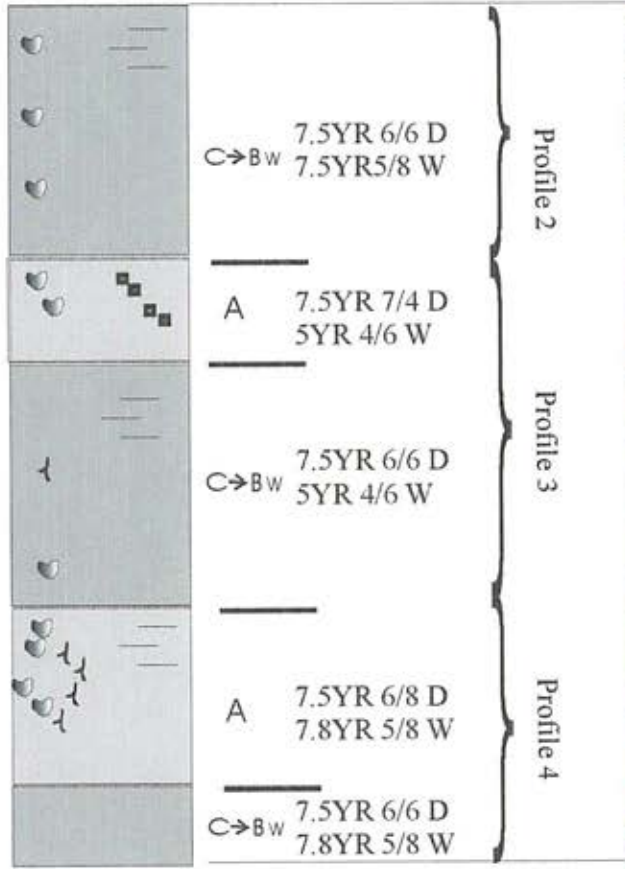
Magnetic Susceptibility of Soil

The nonmagnetic soil has an average susceptibility of 19×10^{-5} S.I. units. With climate and topographic position being the same for both soils, the amount of iron oxide in the nonmagnetic soil is the limiting factor in the production of maghemite. Figure 16 shows the attributes of a typical 2-foot core section of

Nonmagnetic Core 048 (#2)



Horizon Color Profile



Picture



Legend

- Contacts
- Sharp
 - Clear
 - ▣ Gradational
 - √ Roots (in relative abundance)
 - ◐ Chert (in relative abundance)
 - Loose Soil
 - ◑ Poorly consolidated Soil
 - ◒ Well Consolidated Soil
 - ▣ Angular peds
 - ▣ Subangular peds
 - ▣ Platy peds
- Munsell color shown in wet (W) and dry (D)

Figure 16: Diagram of the second core tube extracted outside of the magnetic anomaly showing horizon changes and magnetic susceptibility.

the nonmagnetic soil. Magnetic susceptibility peaks can be seen associated with A/ C→Bw boundaries discussed previously. An exception to this is Profile 4 where the peak is located in the lower part of the C→Bw horizon. Profile 4 is also the thinnest profile, which may result in the deepening of the redox boundary.

Summary

The soil recovered on the ORR from outside anomaly B is a product of colluvium washed down from the top of Copper Ridge. The parent material was derived from extremely weathered soils. The soil shows evidence of A-horizon deflation, accompanied by increasing chert content and a weakening of horizon competence. I have termed the soil located outside the anomaly as an inceptisol. The soil shows strong evidence of hydromorphy and so an aquic suborder is designated. The magnetic soil is rich in iron oxide relative to the nonmagnetic soil. The soil outside the anomaly has an average susceptibility of 19×10^{-5} S.I. units. Susceptibility peaks in the soil are associated with A/ C→Bw boundaries.

Discussion

With the topographic position and climate similar for both soils, I believe the differences in iron content between the two soil cores (the amount of glaeboles) suggest a difference in parent material. Assuming that the original parent rock for both soils is, in part, the underlying Copper Ridge Dolomite, there are two possible explanations for the difference in iron oxide content. The first is

that the parent material of the magnetic soil (alluviums) was subject to long periods of time at or near the water table. Fluctuations in the water table allow for the precipitation and concentration of iron oxides in one area of a soil. The second is a possible outside source of iron, which only influenced the magnetic soil. The most likely source of iron would be the ancient river alluviums, now found on the ridge top due to topographic inversion. If the river carried iron-bearing minerals such as biotite, the pedologic breakdown of these minerals would have increased the iron content of in the parent material. The parent material of the nonmagnetic soil may not be as old and so did not form until after the topographic inversion.

Another possibility is that the nonmagnetic parent material is the same age but was not close enough to the ancient river to be an alluvium, and is rather a residuum of the now eroded ridges, which flanked an ancient river valley. In any case, it is clear that the dolines act as sediment traps collecting material transported by colluvial or alluvial activity on the ridge side. Finally, perhaps streams on the ridge transported the magnetic soil while the nonmagnetic soil was simply colluvium (slope wash). This might help explain the juxtaposition of these very different soils. The fluctuation of the water table within the doline itself may have enhanced the magnetism of soil richer in iron.

CHAPTER 3 LAB ANALYSIS OF SOIL CORES FOR ANOMALY B

Transmission Electron Microscopy

Purpose

TEM (transmission electron microscopy) was employed to determine the morphology, size, and genesis of maghemite crystals found in the magnetic soil on the ORR to help determine whether the maghemite is biologic or abiologic in origin. Magnetite produced by magnetotactic bacteria is usually cubic, octahedral and more rarely prismatic, tooth shaped, arrowhead shaped and bullet shaped. Studies have shown magnetotactic bacteria, that is bacteria which creates intracellular magnetite, produce magnetite crystals ranging from 35-120 nm (Devouard et al., 1998). TEM aids in determining the size of the magnetic particles in the soil core and observing whether their morphologies are consistent with those described in the biologic mechanisms.

Grid Preparation

Material for TEM study was extracted from the soil core using a hand magnet. The extracted particles were placed in vials and the vials marked with a number to denote the soil core from which it was extracted. The place of extraction was then recorded with the number of the extraction.

Part of the magnetic sample was then sonicated in a solution of distilled water for a half-hour. A droplet of this solution was placed on a Petri dish and a 300-mesh copper TEM grid coated with polymer was placed on the surface of the droplet. After a few minutes the grid was removed and excess solution removed from the grid. A droplet of distilled water was then placed on a Petri dish and the process was repeated with the same grid twice using the distilled water only and allowed to dry for 24 hours.

The grid was examined using a Philips EM300 transmission electron microscope. Pictures were taken of the material on the grid and scanned into digital format.

Results

The TEM was unable to aid in the determination of a biotic origin for the maghemite. The reasons for this included an inadequate TEM and the lack of an EDX (energy dispersive X-ray) to be used in conjunction with the TEM. The Philips EM300 used in this phase of the study was only able to focus on crystals larger than 1 micron. To look for biologically created maghemite, magnification would have needed to be great enough to detect crystals on the nanometer scale.

The crystals that were located using TEM were of unknown chemistry as there was no EDX to be used in conjunction with the TEM. Without the chemistry of the particle, I was unable to determine if a particle was an iron oxide. Without this knowledge no conclusions could be made as to the morphology of the maghemite using TEM.

Because the TEM work was ineffective in determining the nature of the

magnetic mineral, SEM (scanning electron microscopy) was employed at ORNL. The SEM at ORNL was equipped with an EDX.

Scanning Electron Microscopy

Introduction

In February, 2002, at Oak Ridge National Laboratory, with the assistance of Dr. Yul Roh of the Environmental Science Division, I used a JEOL JSM-350F SEM to examine mineral grains prepared from both a core removed from inside and outside anomaly B. Pictures of particles illuminated with a beam at a voltage of 19Kv were taken and energy dispersive x-ray analysis (EDX) was used to evaluate the chemistry of the particles. EDX uses an electron beam to dislodge atomic electrons of an element, ionizing the atom. The ionized atoms are neutralized by other electrons and emit x-rays with energies characteristic of the parent atom. The x-rays are collected and used for elemental analysis of a specimen.

EDX figures have a horizontal axis showing x-ray energy levels and a vertical axis showing counts per second of x-rays captured (Appendix 3). EDX does not detect elements lighter than sodium. Therefore, iron-rich particles are thought to be iron oxides as they are the most common iron compounds in soils. The SEM and EDX provided insight into how the soil chemistry varied with depth and particle size within each core, and between the magnetic and nonmagnetic cores.

Sampling

We observed eight samples of soil using SEM (Table 3). Five of the samples were removed from core tubes 1 and 2 of the magnetic core set. These included magnetically separated material from Profile 2, C→B-horizon (sample 1), Profile 3, A-horizon (sample 2) and bulk material from Profile 1, A-horizon (sample 4), Profile 2, A-horizon (sample 5) and Profile 2, C→B-horizon (sample 6). Two samples, one magnetically separated (sample 3) and one bulk (sample 7), were removed from a deeper portion (39 ft) of the magnetic core set to look for variation with depth. One sample (8) was extracted from the nonmagnetic core at a depth of 7 ft for comparison with the magnetic core.

| Sample Number | Sample Description | Sample Weight (Grams) | % Sand and gravel | % Silt and Clay |
|---------------|------------------------------------------------------------------|-----------------------|-------------------|-----------------|
| 1* | Magnetically separated material from Profile 2, C→Bw-horizon | 2.73 | 54.2 | 45.8 |
| 2* | Magnetically separated material from Profile 3, A-horizon | 10.40 | 69.9 | 30.1 |
| 3 | Magnetically separated material removed from core at 39 ft level | 2.48 | 68.1 | 31.9 |
| 4* | Bulk Soil from Profile 1, A-horizon | 10.95 | 16.9 | 83.1 |
| 5* | Bulk Soil from Profile 2, A-horizon | 10.83 | 50.3 | 49.7 |
| 6* | Bulk Soil from Profile 2, C→Bw-horizon | 10.49 | 31.0 | 69.0 |
| 7 | Bulk Soil removed from core at 39 ft level | 10.55 | 33.2 | 66.8 |
| 8 | Bulk soil removed from C→Bw-horizon of nonmagnetic core | 9.39 | 8.8 | 91.2 |

*Extraction point is shown in Appendix 1.

Table 3: Sample numbers, descriptions, and weights of scanning electron microscopy samples. Percentages of silt and clay fraction vs. sand and gravel fraction are also shown.

Sample Preparation

Sand and Gravel

Dr. Roh and I placed the sand and gravel samples in 200 ml shake containers filled to the halfway mark with deionized water. The containers were then placed in a shaker for 24 hours to disaggregate the sand and gravel from the silt and clay, then we sonicated each sample for approximately 1 minute. The sand and gravel fraction of each sample, defined as particles greater than 53 μm (Tarbuck and Lutgens, 2002), was separated using a sieve and deionized water. We then dried the sand and gravel fraction for 2 hours at 105° F before weighing. Magnetic portions of each sample were then removed using a hand magnet and weighed to be mounted on SEM sample holders.

To mount the samples we polished aluminum stub SEM sample holders on one side to remove old sample material and placed double-sided (coated) tape on the polished side. Each sample was given a number that was written on the underside of the sample stub. Only the magnetic portion of the sand fraction was observed using SEM, but original sample names were retained (i.e. a bulk sample is still referred to as a bulk sample even though this separation was done). We placed grains approximately 1 mm in diameter on the tape and observed them under a 40X optical lens. A picture was drawn of the stud and the position of each particle on the stub was then noted, numbered, and a described. The stub was then coated with carbon before being placed into the SEM.

Silt and Clay

Dr. Yul and I were unable to separate the silt and clay fractions. The silt and clay fractions of all but the sample of bulk material from Profile 1, horizon-A aggregated together and settled to the bottom of their containers within minutes of sonication. Sample 4 did not settle over the course of a week and so SEM was not performed on this sample. The remaining samples were dried over 2 days, then stirred into a powder with a spatula.

Because of time restrictions, SEM was performed only on three silt and clay samples: 1, 6 and 8. We made a slurry with the sample material and ethyl alcohol in an attempt to further separate the aggregated particles. A drop of the slurry was then placed on a stub and, after drying, the sample was carbon coated before being placed into the SEM. The slurry did not effectively separate aggregated particles. In spite of this, we studied the samples.

Observations

Sand and Gravel

Sample 1: Seven fragments were observed in this horizon. Six were brownish-red in color; one was black, and all were rounded with a botryoidal surface habit. The fragments were angular to subangular. One of the brownish red particles was high in Si, followed by Fe, Al and Mn (Appendix 3, Figure A3.1) in decreasing order of abundance. This was interpreted as an iron oxide coated chert or quartz fragment, or a small iron oxide nodule heavily coated with silica. Five fragments showed Fe to be the main chemical constituent followed by Si, Al and Mn

(Appendix 3, Figure A3.2). These may be heavily iron oxide-coated chert or quartz fragments, or iron oxide nodules with coatings of silica. One small dome-shaped particle was located that was pure iron oxide (Plate 2, Picture 4 and Appendix 3, Figure A3.3). This was interpreted as a nodule of pure maghemite or magnetite.

Sample 2: Six fragments were observed in this horizon. All were rounded with botryoidal surfaces. Two were red-black and the other four were reddish brown. In five out of the six cases, Fe was the dominant element, followed by Si, Al and Mn in decreasing order (Plate 2, Picture 5). In the sixth case, a red-brown fragment, Si was shown to be dominant, followed by Fe, Al and Mn. (Appendix 3, Figure A3.4).

Sample 3: Eight round and botryoidal fragments were observed from this horizon. All fragments were some combination of brown and black. Three of the four blackest fragments were rich in Si. The samples that appeared to have a greater portion of brown were higher in Fe than other elements. One fragment (Plate 2, Picture 6 and Appendix 3, Figure A3.5) was almost pure iron oxide. I interpret it to be a maghemite nodule, though it is not as rounded as the nodule found in Profile 2, horizon-C.

Sample 4: Eight fragments were observed from this horizon. All were brownish-red in color and two contained black portions. Fragments were round and botryoidal. One of the fragments with a black portion had Fe as its most prevalent element. All the others were highest in Si with lesser amounts of Fe, Al and Mn (Plate 3, Picture 1 and Appendix 3, Figure A3.6).

Sample 5: Seven fragments were observed from this horizon. Six of the seven were reddish brown and one was black. Fragments were both angular and rounded in this horizon. Two showed botryoidal surfaces while others appeared granuloze. Four out of the seven (including the black fragment) were highest in Fe followed by Si, Al and Mn in descending order of abundance. In one case smaller Fe rich fragments were aggregated to a larger one. It is possible the aggregation is due to magnetic attraction (Plate 3, Picture 2 and Appendix 3, Figure A3.7).

Sample 6: Six fragments were observed from this horizon. These fragments had rounded morphologies and all but one had granuloze texture. One fragment was botryoidal with a metallic luster. Four out the six were reddish brown while two were black. One of the black fragments and the metallic botryoidal fragment (which was red-brown) had Fe in greatest abundance followed by Si, Al and Mn. The other fragments were richest in Si followed by Fe, Al and Mn (Appendix 3, Figure A3.8).

Sample 7: Seven fragments were observed from this point in the magnetic soil core. Six were rounded reddish-brown with a granuloze texture and one fragment was a white chert fragment with black crystals on surface. When EDX analysis was performed, only Si and Al were found on the chert. The black crystals observed optically could not be explained, perhapes there was not enough material to yeild an EDX reading. All the other fragments contained Si, Fe, Al and Mn in descending order of abundance, with Al and Mn being almost to equal in abundance (Appendix 3, Figure A3.9).

Sample 8: Eight fragments were observed from 7 ft deep sample in the nonmagnetic soil core. They ranged from rounded to subangular with granulose surfaces. Five fragments were tan to white, two were brown and one was a root. The root (Plate 3, Picture 3 and Appendix 3, Figure A3.10) was silica coated. Fe was the most abundant element in the two brown fragments, which are interpreted as iron oxide nodules. We were unable to separate any magnetic material from this core, therefore the iron oxide is thought to be nonmagnetic. The other tan-white fragments had Si, Al, and Fe in order of decreasing abundance (Appendix 3, Figure A3.11) and are chert or quartz fragments.

Silt and Clay

SEM was used to characterize the silt and clay fraction of samples 1, 6 and 8. In all three cases, no single fragments of Fe rich material could be located. Both the samples from the magnetic core (the bulk and the separated) showed Si to be the most abundant element followed by equal amounts of Al and Fe (Plate 3, Picture 4 and Appendices 3.12 and 3.13). The silt and clay fraction from the nonmagnetic core showed Si to be the most abundant element followed by Al and Fe in order of decreasing abundance (Appendix 3, Figure A3.14).

Discussion

The SEM and the EDX work yielded a picture of a dome shaped particle, with a diameter of about 200 μm and a chemistry of pure iron oxide from sample 2, the magnetically separated material of Profile 2 C \rightarrow B-horizon (Plate 4, Picture 2; Appendix 3, Figure A3.3). Because this particle was part of a magnetically

separated sample set, I am confident that it is magnetite or maghemite.

Mechanisms 3, 5, 7 and 8 all discuss the production of single domain magnetite or maghemite. Single domain magnetite crystals can be no larger than 280 nm (Dunlap and Ozdemir, 1997). Studies have shown magnetotactic bacteria, bacteria that create intracellular magnetite, produce magnetite crystals ranging from 35-120 nm (Devouard et al., 1998). This includes strictly anaerobic bacteria (GS-15 type; mechanism 3) that produce single domain magnetite (Fe_3O_4) particles with diameters less than 50nm (Lovley et al., 1987), and microaerophilic assimilatory (mechanism 5) bacteria that produce chains of single-domain magnetite, magnetosomes with diameters 20-100nm (Fassbinder et al., 1990). The dome shaped particle with a diameter of 200 μm is obviously not single domain and far too large to be produced by such mechanisms. Crystals of magnetite produced by magnetotactic bacteria are usually cubic, octahedral and more rarely prismatic, tooth-shaped, arrowhead-shaped and bullet-shaped (Devouard et al., 1998). Rounded forms are rare and associated with smaller than average magnetotactic crystals (Devouard et al., 1998). The particle found in Profile 2 is very well rounded and does not resemble magnetotactic bacterial magnetite (Plate 2, Picture 4 and Appendix 3, Figure A3.3). Although Mullins (1977) reported that microbial iron reduction (mechanism 7) produced maghemite particles smaller than 100 nm, and similarly Taylor et al. (1987) synthesized particles smaller than 100 nm abiologically (mechanism 8), in principle either mechanism could produce much larger maghemite particles, concretions or

coatings given sufficient time or repeated oxidation-reduction cycles driven by microbes or water table fluctuation.

Particulate matter from pollution sources (flyash) was proposed as a possible source of magnetic material in magnetic soil formation (mechanism 2). Typical flyash is on the order of $1\ \mu\text{m}$ (Tompson and Oldfield, 1986; King et al., 1999) clearly making the particle from Profile 2, C-horizon too large to be flyash. In a study of particulate samples in the United Kingdom, King et al. (1999) found particles no larger than $190\ \mu\text{m}$.

Si, Fe and Al are the three most abundant elements in both the gravel/sand fraction and the silt/clay fraction. In the case of the gravel/sand fraction, most particles varied from predominately Fe-rich (Si coated iron oxide nodules or chert and quartz heavily coated with iron oxides) to Si-rich (Fe coated chert or quartz fragments or iron oxide nodules heavily coated with Si). In rare cases individual fragments were pure Fe oxide and Si and Al oxide. These are presumed to be magnetic/maghemite nodules and chert/quartz fragments, respectively. In the silt and clay fraction, Si was the dominant mineral in all cases, Fe and Al were found as secondary elements. This suggests that the silt/clay fraction is composed of iron-coated clay minerals and quartz fragments without distinct nodules of iron oxide or fragments of chert/quartz.

Finally, soil from the nonmagnetic core had a greater abundance of Si and Al than Fe. The two silt and clay samples from the magnetic core show Fe and Al to be of equal proportion. This implies that the total amount of Fe in the magnetic core is greater than that of the nonmagnetic core in this fraction.

With the use of the SEM and the EDX we have shown that neither magnetotactic bacteria (mechanisms 3 and 5) nor influx of flyash (mechanism 2) were responsible for the production of the magnetic fragments in the magnetic soil core. Most of the iron oxides in the magnetic core exist as coatings rather than distinct particles. Pure Fe particles, when found, are round. In the silt and clay fraction Si is always the dominant element and Fe/Al exist in lesser amounts. In the silt and clay fraction more Fe is present relative to Al in the magnetic core than the nonmagnetic core.

X-Ray Diffraction

Introduction

In February, 2002, at the Oak Ridge National Laboratories, Dr. Yul Roh of the Oak Ridge Environmental Science Division used XRD (X-ray diffractometry) to examine soil samples prepared from both the cores. The purpose of the XRD work was to determine the mineralogy of the soil in the cores. Clay mineralogy is used as a proxy for pH conditions and the amount of leaching in the soil (Birkeland, 1999). XRD data were used to identify the mineral that causes magnetism in the ORR soils, in turn helping us to evaluate the mechanisms of magnetic soil formation.

X-ray diffractometers expose crystalline materials to X-rays. The X-rays are diffracted and the pattern of diffraction is dependent on the nature of the crystalline material. This predictable diffraction pattern is used to identify

crystalline material. Non-crystalline material, such as amorphous oxides, cannot be identified using XRD.

Dr. Roh recorded that "Sand fractions were ground with hand-pressure for 5 minutes with an agate mortar and pestle. Duplicate boxed mounts (Jackson, 1975) were made of the ground sand fractions as well as silt plus clay fractions. All XRD analyses for mineralogical characterization were performed with a Scintag XDS 2000 diffractometer (Scintag, Sunnyvale, CA) operating at a scan rate of $2^\circ 2\theta/\text{min}$. Cobalt K- α radiation ($\lambda = 1.79026\text{\AA}$) was used for the XRD analyses" (personal communication with Dr. Yul Roh, Oak Ridge National Laboratory, 2002).

Sampling

Dr. Roh analyzed eight samples of soil using XRD (Table 4). Five of the samples were removed from core tubes 1 and 2 of the magnetic core. These included magnetically separated material from Profile 2, C \rightarrow B-horizon (sample 1), Profile 3, A-horizon (sample 2) and bulk material from Profile 1, A-horizon (sample 4), Profile 2, A-horizon (sample 5) and Profile 2, C \rightarrow B-horizon (sample 6). Two samples, one magnetically separated (sample 3) and one bulk (sample 7), were removed from a deeper portion (39 ft) of the magnetic core to look for variation with depth. One sample (8) was extracted from the nonmagnetic core at a depth of 7 ft for comparison with the magnetic core.

The samples were separated into sand and gravel fractions as well as silt and clay fractions using the same methods described in the SEM section. Due to

time restrictions, XRD was not performed on the sand and gravel fractions of the bulk soil samples.

Results

The results of the analysis are summarized in Table 4. Quartz was found in every sample. The presence of quartz is not surprising as it is abundant

| Sample Number | Sample | Minerals found in Sand and Gravel Fraction | Minerals found in Silt and Clay Fraction |
|---------------|------------------------------------------------------------------|--------------------------------------------|------------------------------------------|
| 1* | Magnetically separated material from Profile 2, C→Bw-horizon | Quartz, maghemite, hematite | Kaolinite, quartz |
| 2* | Magnetically separated material from Profile 3, A-horizon | Quartz, maghemite, hematite, calcite | Kaolinite, quartz, maghemite, hematite |
| 3 | Magnetically separated material removed from core at 39 ft level | Quartz, maghemite, hematite | Kaolinite, quartz, maghemite, hematite |
| 4* | Bulk soil from Profile 1, A-horizon | NA | Quartz |
| 5* | Bulk soil from Profile 2, A-horizon | NA | Kaolinite, quartz |
| 6* | Bulk soil from Profile 2, C→Bw-horizon | NA | Kaolinite, quartz |
| 7 | Bulk soil removed from core at 39 ft level | NA | Kaolinite, quartz |
| 8 | Bulk soil removed from C→Bw-horizon of nonmagnetic core | Quartz, maghemite, hematite | Illite, kaolinite, quartz, maghemite |

*Extraction point is shown in Appendix 1.

Table 4: Minerals identified using x-ray diffraction.

on the Earth's surface and is resistant to weathering. Quartz was found in every thin section and detected in every EDX reading (see SEM section).

Kaolinite, found in the silt and clay fraction of all samples except Profile 1, A-horizon (sample 4), is a clay mineral commonly found in highly weathered soils. It is rich in SiO_2 and Al_2O_3 , both of which are resistant to weathering (Birkeland, 1999). Because these soils were subjected to high amounts of precipitation, the presence of kaolinite is expected. The lack of kaolinite in sample 4 points to a different source for this material. Unlike all the other A-horizons in the magnetic core, this A-horizon was rich in silt, poor in sand and gravel, and lacked an abundance of chert (<5%). I speculate that the parent material was loess.

Maghemite and hematite were found together in every sand and gravel fraction, and in silt and clay fractions from magnetically separated material from Profile 3, A-horizon (sample 2); magnetically separated material removed from magnetic core 39 ft deep (sample 3); and bulk soil removed from C→Bw-horizon of nonmagnetic core (sample 8). It is interesting to note that maghemite did form in the nonmagnetic core. This shows that the redox conditions needed for the creation of maghemite existed in both soils. The lack of iron bearing minerals in the silt and clay fraction of the bulk magnetic samples suggest that the iron oxides in this fraction are amorphous.

The presence of illite probably is evidence of the presence of weathered mica that is breaking down into clay. Illite and mica have very similar properties (Birkeland, 1999). Mica probably could not have come from the underlying dolostone and is evidence of an ancient alluvial sediment source.

The calcite present in the magnetically separated material from Profile 3, A-horizon may be relict from the dolomite bedrock. The calcite may have been inside a chert nodule and exposed when the sample was ground. I would not expect to find calcite otherwise, as it is an easily weathered and leached mineral.

Summary

The XRD work performed by Dr. Roh shows the soils to be rich in quartz, and kaolinite. Because these minerals are resistant to weathering and weatherable minerals are absent in the soil, the soil is interpreted as being highly leached. The mineral maghemite is interpreted as the cause of magnetism in the ORR soils in agreement with others (Hatcher et al., 1992; Kopp and Lee, 1987). The presence of calcite is probably relict from the underlying bedrock. The presence of illite supports the hypothesis of a magnetic soil parent material which includes ancient alluvium.

CHAPTER 4 DISCUSSION AND CONCLUSIONS

Evaluating the Mechanisms of Magnetic Soil Formation

X-ray diffraction performed by Dr. Yul Roh at ORNL confirmed earlier work (Hatcher et al., 1992; Kopp and Lee, 1987) that found maghemite is the mineral causing the magnetism of the ORR soils. In chapter 1, I listed nine mechanisms for the magnetic enhancement of soils. I now discuss each of them in light of the data presented in this thesis.

1) *Long term weathering and pedogenesis that concentrates primary residual ferrimagnetic minerals.* Helm (1995) showed the underlying rock to be nonmagnetic (5×10^{-5} S.I), so it is unlikely that iron in the dolomite is in a highly magnetic form. This interpretation is supported by Moukarika et al. (1991) who studied magnetic soils formed on dolomite. They determined that the dolomite supplied the iron to the magnetic soil in the form of hematite and goethite, but that the soil magnetism was due to later transformation of these oxides into maghemite. Both the Copper Ridge and Chestnut Ridge are underlain by Copper Ridge Dolomite. Copper Ridge contains many more magnetic anomalies than does Chestnut Ridge. If the soil magnetism was due to primary weathering of the Copper Ridge Dolomite, I would expect the two ridges to have a similar density of magnetic anomalies. The possibility of magnetic enhancement of the soil due to the weathering of a magnetic parent material can be rejected.

2) *Accumulation of relatively coarse (>1 μm) airborne magnetic particulates mainly from pollution sources.* Typical flyash is on the order of 1 μm (Tompson and Oldfield, 1986; King et al., 1999). In a study of particulate samples in the United Kingdom, King et al. (1999) showed particulates up to 190 μm. The two pure iron oxide particles located using SEM that are greater than 200 μm (Plate 2, Pictures 4 and 5) and are too large to be flyash. Furthermore, if flyash were the cause of the magnetic enhancement, I would expect to see the largest magnetic susceptibility in the uppermost A-horizon, with the strength of the signal fading with depth. The depth of the magnetic signal in the soil cores (200 x 10⁻⁵ S.I. to more than 50 ft) and the distribution of the magnetic signal with depth showing peaks at the bottom of buried A-horizons does not support the hypothesis of flyash as a source of magnetic enhancement.

3) *Strictly anaerobic bacteria that produce single domain magnetite (Fe₃O₄) grains with diameters <50nm.* The two pure iron oxide particles located using SEM were far too large to be produced by bacteria (Plate 2, Pictures 4 and 5). The roundness of these particles does not fit the description of magnetite produced by magnetotactic bacteria. These are usually cubic, octahedral and more rarely prismatic, tooth-shaped, arrowhead-shaped, and bullet-shaped. Rounded forms are rare and associated with smaller than average magnetotactic crystals (Devouard et al., 1998). Finally, the association of the peak magnetic susceptibilities with the A-horizon (oxidized) makes it unlikely that anaerobic bacteria was a major source of magnetic enhancement.

4) *Anaerobic formation of greigite (Fe_3S_4) linked to microbial reduction.*

Stanjek et al. (1994) show greigite to form at a depth of 2.5 ft in a gley soil (which is reduced) as a result of sulfate reduction due to anaerobic respiration. Magnetic enhancement on the ORR is associated with oxidized horizons. In Stanjek et al.'s study, sulfate was supplied by pyrite in the parent rock. On the ORR, pyrite has not been reported in the underlying Copper Ridge Dolomite. Most importantly, maghemite has been shown by XRD to be the magnetic carrier mineral.

5) *Microaerophilic assimilatory bacteria (magnetotactic bacteria) that produce chains of single-domain magnetite magnetosomes with diameters 100-220nm.*

Essentially, the same problems exist with this mechanism as with mechanism 3. The magnetic iron oxide particles located using SEM (Plate 2, Pictures 4 and 5) are too large and too round to support this mechanism. Furthermore, these bacteria thrive in reducing conditions, where the highest magnetic signal in the ORR soils is associated with oxidized horizons.

6) *Thermal transformation of weakly magnetic iron oxides and hydroxides to ferrimagnetic magnetite or maghemite by natural fires or crop burning in the presence of organic matter.*

Dearing et al. (1996) showed that annual fires over the course of hundreds of years do not produce strong signals in comparison to fire pits. Further, experiments by Dearing et al. (1996) showed "no significant differences after 8 years of annual burning" when compared with adjacent unburned plots.

Additionally, the depth and distribution of the magnetic signal would not seem to support this process. If fire caused the magnetism, I would expect

magnetic soils to be ubiquitous and not confined to the bull's-eye pattern seen on the ORR. The depth of the magnetic signal (greater than 50 ft) does not support the hypothesis of a magnetization process that occurs at the surface. However, it is possible that alluviums from Copper Ridge were washed into dolines and subsequently heated before being buried by new alluvial colluvium. But, the fire would affect soils formed both inside and outside the doline and cannot account for the magnetic bull's-eye patterns. Direct evidence that the magnetism is not a result of burning comes from the EDX figures associated with the two magnetic spherules found in the magnetic soil (Plate 2, Pictures 4 and 5). Maher and Taylor (1988) noted that that transformation of goethite and hematite to magnetite during burning usually results in Al substituted magnetic minerals. No such substitution was detected in these particles.

9) *Fulgurites (formations caused by lightning strikes)*. I would expect the fulgurite mechanism to create bull's-eye anomalies, but I would not expect any magnetic transformation caused by a single strike to extend more than 50 ft deep. To explain the susceptibility peaks in the soil core, lightning would have to strike the surface of the doline before each subsequent burial. It seems unlikely that lightning would a doline preferentially. Furthermore, I do not see in thin section the vesicular glass relicts created by the fusing of silica during the strikes.

Two hypotheses remain viable after our analysis. They are:

7) *Anaerobic microbial Fe reduction followed by formation of single-domain magnetite or maghemite ($\gamma\text{Fe}_2\text{O}_3$) grains with diameters $<100\text{nm}$.*

and

8) *Abiological weathering of the Fe(III) bearing minerals followed by oxidation leading to magnetite or maghemite, as demonstrated in synthetic experiments (Taylor et al., 1987).*

One or both of these mechanisms is probably responsible for the magnetic enhancement of soils on the ORR. Essentially, these two mechanisms are the same, creating maghemite through redox cycles. The only difference between them is the reducing agent. In mechanism 7 the reducing agent is microbial and in mechanism 8 it is abiological (water table fluctuations). The morphology and size of the magnetic particles created by these two mechanisms are indistinguishable, consequently it is not possible to know which mechanism is responsible for the magnetic enhancement of the soil. Because the agents of these mechanisms both exist on the ORR, it is probable that they work in tandem. Although Mullins (1977) reported that microbial iron reduction (mechanism 7) produced maghemite particles smaller than 100 nm, and similarly Taylor et al. (1987) synthesized particles smaller than 100 nm abiotically (mechanism 8), in principle either mechanism could produce much larger maghemite particles, concretions or coatings given sufficient time or repeated redox cycles.

Out of 14 profiles identified in the two soil cores, 10 showed increased magnetic susceptibility at or near the bottom of the A-horizon. The spikes are evidence of relict redox boundaries of now buried soils. Lower in the core the

magnetic susceptibility drops, reflecting the dissolution of maghemite caused by the prevailing reducing environment. There is no XRD evidence that the dissolved iron precipitates into another crystalline form. What iron comes out of solution at depth likely forms an amorphous iron oxide unidentifiable with XRD. The susceptibility pattern seen in the cores is a reflection of the cyclic redox environment optimal for the creation maghemite by mechanisms 7 and 8, while mechanisms that require strictly reducing conditions (mechanisms 3, 4, and 5) are inapplicable to the ORR soils.

Sources of Iron

The soils recovered in cores taken from inside and outside of anomaly B are both the product of old parent material, have similar topographic position, and have been exposed to the same weathering processes. Both soils, therefore, were subjected to the same external conditions that enhanced magnetic susceptibility of the soil inside the anomaly. Supporting this are the XRD data, which show maghemite exists in the soil outside of the anomaly. The differences in magnetic susceptibility between the two cores are due to differences in iron content. The more iron available for transformation to a magnetic oxide, the higher the susceptibility of the soil.

There is a record of magnetic soils developing on iron poor parent material (Dearing et al., 1996; Moukarika, et al. 1991). Moukarika et al. (1991) described a magnetic soil that developed on a ferroan dolomite. The development of the soil involved the dissolution of the magnesium carbonate over time leaving behind materials resistant to chemical weathering. In this way parent rock poor in

iron can underlie soil rich in iron. Redox conditions in the iron-rich soil then lead to the formation of maghemite. On the ORNL Phillips et al. (1998) showed that soils relatively rich in iron (2-4%) developed over inter-layered shale and limestone bedrock with only trace amounts of iron (<0.3 %) through the same process as described by Moukarika et al. (1991). Studying Californian magnetic soils, Singer and Fine (1989) showed that the magnetic susceptibility of soils in California increased with precipitation. This may be a result of the redox cycles needed to produce maghemite and the frequency of reducing conditions created by the precipitation. I believe it to also be a function of the removal of less resistant parent material concentrating the remaining iron oxide. Singer and Fine (1989) went on to show that the older the soil the more magnetic the soil became. More time results in greater iron concentration.

According to soil maps provided by the Oak Ridge Restoration Project and the Status Report on the Geology of the Oak Ridge Reservation (Hatcher et al., 1992), the parent material of the magnetic soil is ancient alluvium found at the crest of Copper Ridge. Support for this interpretation is found in the quartzite cobble from the magnetic soil (Plate 1, Picture 5). According to Phillips et al. (1998) and Crownover (1994) cobbles of metaquartzite are evidence of ancient alluviums that were deposited by rivers that flowed from the Unaka Mountains or Clinch Mountain. How much of the extracted magnetic soil is original alluvium and how much is Copper Ridge residuum is unclear, but undoubtedly the two mixed during colluviation.